Chem Soc Rev

REVIEW ARTICLE

View Article Online
View Journal

Cite this: DOI: 10.1039/d3cs00736g

Contact-electro-catalysis (CEC)

Ziming Wang,[ab] Xuanli Dong,[ab] Wei Tang [ab] and Zhong Lin Wang *[abc]

Received 13th December 2023

DOI: 10.1039/d3cs00736g

rsc.li/chem-soc-rev

Contact-electro-catalysis (CEC) is an emerging field that utilizes electron transfer occurring at the liquid–solid and even liquid–liquid interfaces because of the contact-electrification effect to stimulate redox reactions. The energy source of CEC is external mechanical stimuli, and solids to be used are generally organic as well as in-organic materials even though they are chemically inert. CEC has rapidly garnered extensive attention and demonstrated its potential for both mechanistic research and practical applications of mechanocatalysis. This review aims to elucidate the fundamental principle, prominent features, and applications of CEC by compiling and analyzing the recent developments. In detail, the theoretical foundation for CEC, the methods for improving CEC, and the unique advantages of CEC have been discussed. Furthermore, we outline a roadmap for future research and development of CEC. We hope that this review will stimulate extensive studies in the chemistry community for investigating the CEC, a catalytic process in nature.

1. Introduction

Catalysis has played a pivotal role in the advancement of human society owing to its profound significance in industrial processes and environmental sustainability.[1–6] Substantial efforts have been devoted to gaining a comprehensive understanding of the fundamental mechanisms underlying catalysis.[7–12] These efforts have, in turn, driven the development of catalytic strategies with exceptional performance.[13–19] Within the spectrum of established catalytic techniques, mechanocatalysis has attracted extensive attention, primarily due to its distinct advantages such as enhanced energy efficiency and diminished environmental impacts.[20–25] Force-induced increase of defects,[26,27] extreme conditions,[28,29] or other effects[30,31] are three governing operating mechanisms for conventional mechanochemical processes. However, the contribution of the contact-electrification (CE) effect to mechanochemistry has been largely ignored, despite the fact that mechanical stimuli would inevitably result in frequent contact-separations between friction pairs. A series of studies have provided compelling evidence that electrons serve as the primary charge carriers in a majority of CE cases,[32–39] and the high-intensity electric field at the contact surfaces could facilitate the electron transfer as well as motivate the subsequent redox

[a] CAS Center for Excellence in Nanoscience, Beijing Institute of Nanoenergy and Nanosystems, Chinese Academy of Sciences, Beijing, 100140, China. E-mail: zhong.wang@mse.gatech.edu
[b] School of Nanoscience and Engineering, University of Chinese Academy of Sciences, Beijing, 100049, China
[c] School of Materials Science and Engineering, Georgia Institute of Technology, Atlanta, GA 30332-0245, USA

Ziming Wang

Ziming Wang is currently a post-doctoral research fellow at the Beijing Institute of Nanoenergy and Nanosystems, Chinese Academy of Sciences. He received his PhD degree in condensed matter physics from the University of Chinese Academy of Sciences (UCAS), under the supervision of Prof. Zhong Lin Wang. His research interests include contact-electro-catalysis, self-powered sensors, and energy harvesting.

Xuanli Dong

Xuanli Dong received his bachelor's degree from Beijing Information Science & Technology University in 2020. He is currently pursuing his PhD degree in Beijing Institute of Nanoenergy and Nanosystems, Chinese Academy of Sciences. His research focuses on contact electrification at the liquid–solid interface and contact-electro-catalysis.

reactions,[40–44] further verifying the feasibility of catalyzing chemical reactions through the CE effect. In this context, contact-electro-catalysis (CEC) has been proposed as a bridging concept that connects CE with mechanochemistry, and has been demonstrated to be a significant supplement to existing catalytic strategies.

Contact-electro-catalysis (CEC), first proposed in 2022, is an emerging field that utilizes CE-driven electron exchange at the liquid–solid and even liquid–liquid interfaces to stimulate redox reactions.[45] The energy source of CEC is external mechanical agitations, and the solid to be used is general organic[46] (such as FEP and PTFE) and inorganic materials[47] (such as SiO_2, Al_2O_3, *etc.*) despite they are chemically inert. This paradigm-shift technology opens up exciting possibilities for the development of innovative catalysts and catalytic processes. Distinguished from conventional catalytic strategies that impose specific requirements on their catalysts, CEC paves the way for virtually any material to serve as a catalyst as long as it demonstrates satisfactory CE capabilities. For instance, commercially available pristine polymers can catalyze the production of reactive oxygen species (ROS) through CEC,[45,48–50] even though they are considered as chemically and catalytically inert. Thus, the range of materials that can be envisaged as catalysts could be considerably expanded due to the ubiquity of CE. Besides, CEC is highly consistent with the principle of green chemistry partly because the driving force is readily available but often wasted mechanical energy, which is beneficial for reducing the dependence on fossil fuels or electricity. As a consequence, CEC could not only eliminate the utilization of noble metals and environmentally harmful chemical reagents during synthesis of catalysts, but also lead to substantial reductions in carbon emissions during the catalytic process. More importantly, CEC offers considerable opportunities for coupling with other catalytic mechanisms, and we expect their synergistic effects could render a substantial enhancement in catalytic efficiency. On the one hand, CE is a ubiquitous surface phenomenon that remains largely independent of the bulk property of materials.[51–53] This merit has enabled diverse methods for integration such as using high CE-ability materials for fabricating reaction chambers or appropriate surface modifications for enhancing the CE performance of employed catalysts. On the other hand, CE-induced electrons on the surface could not only directly catalyze target reactions, but also provide a high-intensity electric field that may promote the separation of charge carriers within existing catalysts for achieving a substantially improved catalytic efficiency.

These prominent features endow CEC with unique advantages in practical applications. CEC might be the potential mechanism for illustrating why the running water does not rot since the CE phenomenon during the flow of water could catalyze the production of ROS for degrading organic pollutants.[45] Besides, CEC has enabled direct synthesis of H_2O_2 under ambient conditions and even anaerobic conditions with rather low cost, no harmful intermediates or byproducts, and the potential for scalable production.[48] The third representative application of CEC focuses on recycling cathode materials in spent lithium-ion batteries (LIBs).[54] High leaching efficiencies of both Co and Li were achieved under mild conditions without using toxic and expensive inorganic strong acids, which could not only simplify the process of waste management, but also enable considerable economic benefits. Moreover, we envision that CEC could also be applied in the research field of biological sciences such as for cancer therapy and longevity studies, which are closely related to the production of ROS.[55–58]

In this review, we will introduce the fundamental principle, prominent features, and significant applications of CEC. We hope this review will provide the reader with a comprehensive understanding and an extensive overview of the vital role of contact-electro-catalysis as well as inspire more insightful opinions in addition with significant breakthroughs in this field (Fig. 1).

Wei Tang

Wei Tang received his B.S. degree from the Physical Department and PhD degree from the Microelectronic Department of Peking University in 2008 and 2013, respectively. He is a professor at the Beijing Institute of Nanoenergy and Nanosystems, Chinese Academy of Sciences. His research interests include interface electron transfer and its applications in wearable electronics, contact-electro-catalysis, and energy harvesting devices.

Zhong Lin Wang

Zhong Lin Wang received his PhD degree in Physics from Arizona State University. He is the Director of the Beijing Institute of Nanoenergy and Nanosystems and Regents' Professor and Hightower Chair at the Georgia Institute of Technology. He pioneered the nanogenerators field for distributed energy, self-powered sensors, and large-scale blue energy. He coined the fields of piezotronics and piezophototronics for third-generation semiconductors. Among 100 000 scientists across all fields worldwide, he is ranked #5 in Career Scientific Impact, #1 in Nanoscience, and #2 in Materials Science. His Google scholar citation is over 400 000 with a h index of over 300.

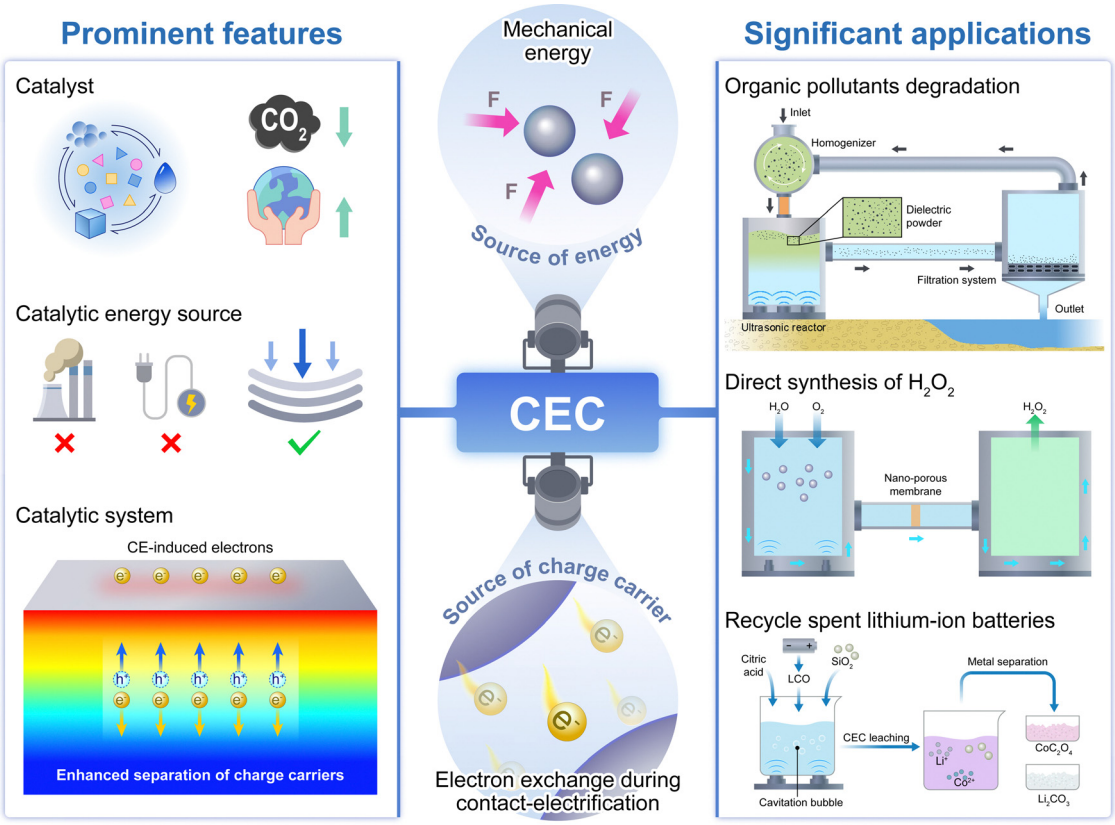

Fig. 1 Schematic illustration of the fundamental principle, prominent features and significant applications of contact-electro-catalysis (CEC). Reproduced with permission from ref. 45, 48, and 54. Copyright 2022, Springer Nature and Wiley.

2. Fundamentals of contact-electro-catalysis

2.1. Electron transfer during contact-electrification

Contact-electrification (CE) is a ubiquitous effect that exists among a variety of interfaces.[59–61] In addition to the well-known CE phenomenon at solid–solid interfaces,[53,62,63] CE can also take place when a liquid contacts with a solid.[32,34,64] The two contact surfaces after CE are reversely charged, and previous studies on liquid–solid (L–S) CE have ascribed the charge transfer process solely to ion transfer that results from ion adsorption or ionization reactions.[32,65] However, a series of recent investigations have proved the existence of electron transfer during CE at L–S interfaces, and, in some cases, electron transfer appears as the dominant process.[32,66] An "electron-cloud-potential-well" model has been proposed to illustrate the mechanism of electron transfer during CE, which assumes that the overlap of electron clouds due to contact under mechanical stimuli is the driving force for interfacial electron transfer.[38] Specifically, the liquid will collide with the solid driven by thermal motion or fluid pressure, which is capable of inducing the overlap of the corresponding electron clouds for electron exchanging. Based on the electron exchange process between different substrates in a typical catalytic process, we suppose that the contribution from the CE effect to promote chemical reactions might be ignored.

In this section, we first introduce the recent progress in electron transfer during L–S CE and its impact on the liquid–solid interfaces. Afterwards, the feasibility of using the CE effect to catalyze chemical reactions is discussed by comparison with several well-established heterogeneous catalytic strategies. The concept of contact-electro-catalysis (CEC) and its prominent feature have been elucidated by summarizing the broad selection range of catalysts and strategies for initiating CEC. The "two-step" mechanism and the rate determining step of producing reactive oxygen species (ROS) by CEC have also been discussed for better understanding the underlying principle of CEC. At last, the factors influencing the CEC efficiency and the corresponding strategies for further improvement are presented.

2.1.1. Evidence of contribution from electron transfer to L–S CE. Various strategies have been developed for the investigation of contact-electrification (CE) at liquid–solid (L–S) interfaces in recent years. By sandwiching a droplet between two solid films, Nie *et al.* have proposed a controllable strategy to quantify the transferred charges during L–S CE.[33] The CE was induced by applying an external force on films to squeeze the droplet, and the contact area between the droplet and the solid films could thus be modulated by applying different pressures, as described in Fig. 2a. The quantity of charges on the droplet after CE was measured using an electrometer. As one of the most representative L–S CE cases, the CE between the deionized (DI)

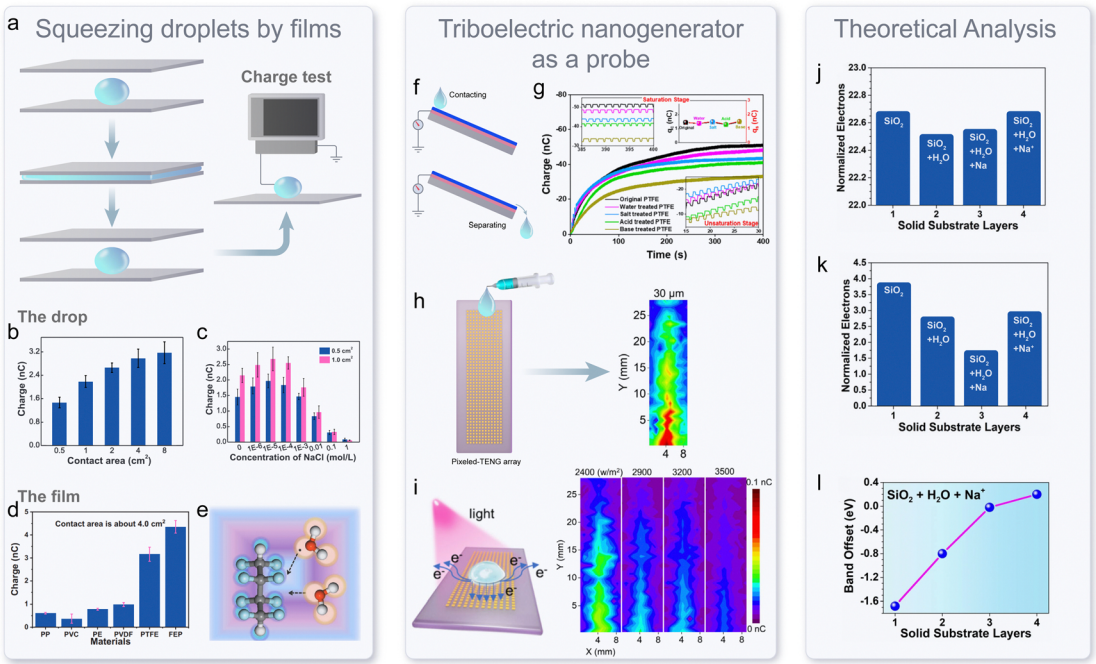

Fig. 2 Investigations on contact-electrification at liquid–solid interfaces. (a) Schematic of measuring the quantity of charge on a droplet after L–S CE by squeezing it with two films. Measured charge quantities of a water droplet (b) or a droplet containing various concentrations of NaCl (c) after it contacts with the PTFE film and the corresponding mechanisms. Reproduced with permission from ref. 33. Copyright 2020, Wiley. (d) Measured charge quantity when a droplet was squeezed by different polymeric films. (e) Simulated distribution of electron clouds when PTFE chains contact with water molecules. Reproduced with permission from ref. 70. Copyright 2020, Wiley. (f) Schematic illustration for studying L–S CE based on a SE-TENG. (g) Transferred charges during CE between water droplets and the original PTFE or the treated PTFE. Reproduced with permission from ref. 36. Copyright 2020, American Chemistry Society. (h) Schematic of a pixeled TENG array and obtained mapping image of transferred charge density. (i) Illustration of ultraviolet irradiation for emitting electrons and the corresponding mapping images under various light intensities. Reproduced with permission from ref. 66. Copyright 2023, American Chemistry Society. The quantity of normalized electrons in the valence bond (j) and a small range near the Fermi level (k) of SiO_2. (l) Calculated band offset of SiO_2 when Na ions are introduced. Reproduced with permission from ref. 90. Copyright 2021, Springer Nature.

water and a polytetrafluoroethylene (PTFE) film was first investigated. The results shown in Fig. 2b indicate that the measured charge of the DI water droplet exhibits an increasing trend as the contact area expands, reaching approximately 3 nC when the contact area is 8 cm^2. It is important to note that this charge transfer process is likely dominated by electrons since the calculated charge amount would be only 0.15 nC if all these charges were contributed by ion transfer. This is also in accordance with the fact that only traces of ions are contained in DI water. To examine the impact of ions on L–S CE, the DI water was replaced by NaCl aqueous solutions with varying concentrations. As shown in Fig. 2c, the quantity of transferred charges first increases, and peaks when the concentration of NaCl is 10^{-5} mol L^{-1}. A further increase in the NaCl concentration leads to less transferred charges and eventually approaches zero at a NaCl concentration of 1 mol L^{-1}. The charge transfer process when PTFE contacts with DI water is different from the process when it comes into contact with NaCl aqueous solution, which can be partly attributed to the duality of ions. On the one hand, the free ions in the solution would prohibit the electron transfer by the screen effect and most ions will flow with liquids[67–69] On the other hand, a slight increase of the ion concentration in DI water would promote the ion transfer process, and ion transfer also contributes to the charge transfer process during CE. Therefore, the quantity of transferred charges first increases with an appropriate increase of the NaCl concentration (within 10^{-5} mol L^{-1} in this case), and then decreases with further increase of the NaCl concentration. Other effects that result from varied ion concentrations may also influence the L–S interface and subsequent CE process, contributing to the non-linear variation of transferred charges. In addition to studies from the aspect of liquids, Li *et al.* have investigated the contribution of functional groups on solid films to L–S CE.[70] The experimental setup remained the same except that PTFE was substituted by a series of polymers characterized by similar main chains but different functional groups at side chains. The transferred charges between DI water droplets and various polymer films during CE are shown together in Fig. 2d. In general, polymers containing fluorine (F) exhibit superior CE abilities compared to others, and a higher density of F-groups in the side chain leads to an increased quantity of transferred charges. This could be ascribed to that F is a strong electron-

withdrawing (EW) functional group during CE (Fig. 2e).[71–73] The order of EW abilities among investigated functional groups is believed to be $CH_3 < H < OH < Cl < F$.

In virtue of broad material selection ranges and various operating modes,[74–76] the triboelectric nanogenerator (TENG) technique represents a powerful platform for studying L–S CE,[36,77,78] especially for *in situ* investigations. By customizing a PTFE-based single-electrode mode TENG (SE-TENG), Zhan *et al.* have examined the detailed charge transfer process between the water droplets and the PTFE films during CE.[36] Liquids were released drop-by-drop for sliding off the PTFE film, and a Cu electrode on the backside was connected to an electrometer in the ground mode (Fig. 2f). According to the operating principle of TENGs, variation of charge quantities on the PTFE surface will induce corresponding flow of electrons between the Cu electrode and the ground.[62,79,80] Thus, the charge transfer process of CE could be monitored by the output of the SE-TENG. Results shown in Fig. 2g indicate that the PTFE surface accumulated negative charges and reached saturation at around −51 nC after repeated contact with water droplets. To identify the contribution from electron transfer, a series of soaking-dropping experiments have been performed. Fresh PTFE films were immersed in different aqueous solutions for a sufficiently long time before contacting with DI water, which could deposit as many ions as possible on the PTFE surface. However, the total amount of transferred charges for CE in base-treated PTFE still reaches around 70% of that in original PTFE, even though the treated surface is supposed to be saturated with hydroxide ions (OH^-). This result implies that electrons participate in the charge transfer process since the ion transfer should be greatly suppressed by the ion-rich surface of base-treated PTFE. Moreover, by replacing the bulk Cu electrode with a pixeled Cu electrode array in TENGs, Zhang *et al.* have firstly *in situ* investigated the dynamic charge transfer behavior of CE.[66] The electric output of each Cu electrode was independently acquired using a synchronous multi-channel acquisition system and processed according to their time sequence. Thus, the charge distribution on solid films during the movement of DI water droplets could be mapped in almost real-time with a spatial resolution of 0.4 mm and a time sensitivity of 0.02 s (Fig. 2h). Exemplified by CE between DI water and fluorinated ethylene propylene (FEP), Zhang *et al.* have found that charges are not uniformly distributed on the FEP film after CE. The quantity of transferred charges increases along with the sliding of the water droplets, which should mainly be ascribed to the evolution of sliding velocity of droplets.[81] Less ions would be adsorbed on the solid surface if the droplet moves faster on the membrane,[82] which could improve the electron transfer and the amount of transferred charges by diminishing the screen effect. The existence of electron transfer was further confirmed *via* the ultraviolet light irradiation strategy. Electrons are supposed to be excited from dielectric surfaces through photoelectron emission, while ions should remain on the surface.[83] As depicted in Fig. 2i, the quantity of residual charges on the FEP surface decreases with the increase of UV light intensity, verifying that electrons contribute to the charge transfer process of CE between the DI water and FEP.

In addition to these experimental observations, theoretical calculations have also confirmed the existence of electron transfer during CE.[84–88] Willatzen *et al.* have developed a quantum-mechanical model for L–S CE without considering ion transfer.[89] The obtained results suggest that electron transfer alone is sufficient for supporting CE at L–S interfaces. A more detailed quantified model for L–S CE has been proposed by Sun *et al.* based on density functional theory (DFT).[90] The solids in this study are oxide materials, and the liquid is pure water with/without Na ions. The introduction of Na ions is aimed for investigating the impact from ion concentrations. The contribution from electron transfer is evaluated using the quantity of normalized electrons in both the valence band (VB) and a small range near the Fermi level (E_f) of solids. Exemplified by CE between SiO_2 and water, significant changes in electron numbers were observed in both the VB (Fig. 2j) and adjacent region of E_f (Fig. 2k) when oxides contact with water, proving the contribution of electron transfer to CE. Besides, as depicted in Fig. 2l, a noticeable band offset was obtained after the introduction of Na ions, suggesting that ion concentrations would greatly affect the electron transfer process for CE. The consistency between the experimental observations and the electron transfer-based theoretical calculations further suggests the existence of electron transfer during CE.

2.1.2. Dominant role of electron transfer during L–S CE. The dominant role of electron transfer during L–S CE was further elucidated by leveraging the difference in thermal behavior between electrons and ions.[32] Fig. 3a illustrates a detailed protocol for quantifying the ratio of electron transfer during CE at liquid–solid interfaces by Kelvin probe force microscopy (KPFM). The solid film was first fully rinsed by liquid droplets, and then fixed at a heater for measuring the evolution of surface charges at various temperatures. According to the theory of electron thermionic emission, electrons are supposed to be excited and emitted from the solid surface as the temperature increases, while ions are more likely to remain on the original surface.[35,37] Experimental results concerning CE between SiO_2 and DI water in Fig. 3b corroborate this assumption. Electrons dominate the charge transfer process during the initial contact with DI water since a noticeable decay in surface charge density was observed during the heating procedure. The ratio of electron transfer could be quantified by assuming that the decreased surface charges correspond to electrons, while the residual charges correspond to ions. A stable surface charge density was obtained after repeat contact-heat cycles, which should mainly be ascribed to the saturation of ions on the SiO_2 surface that result from the thermionic emission of electrons.

Another distinguishing characteristic between electrons and ions is that the electron is spin-conservative and should follow the Pauli exclusion principle during transitions.[91–93] Based on this feature, Lin *et al.* have applied a magnetic field to regulate the spin configuration of unpaired electrons in radical pairs and examined its correlation with the charge transfer process during L–S CE.[64] Fig. 3c depicts the layout of the experimental setup.

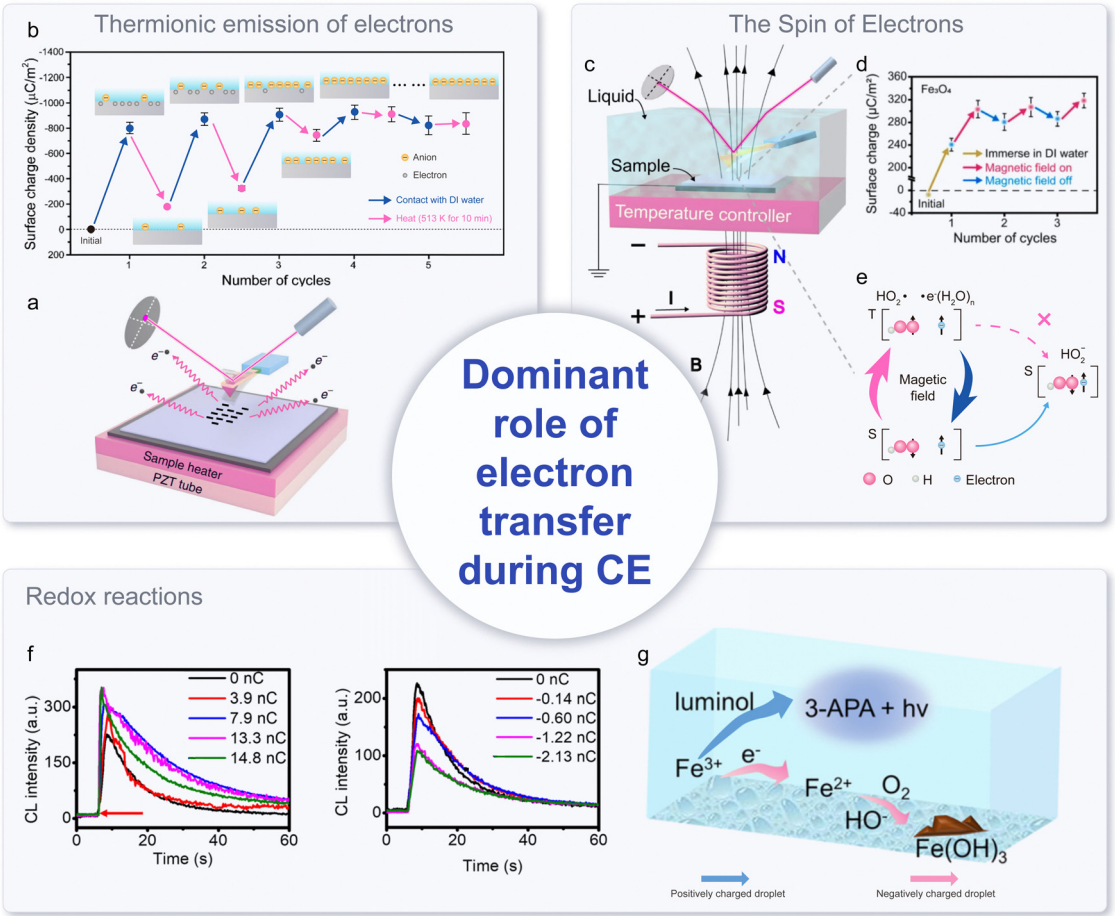

Fig. 3 Revealing the dominant role of electron transfer in liquid–solid contact-electrification. (a) Experimental setup for quantifying the ratio of electron transfer through thermionic emission. (b) Evolution of surface charge density on the SiO_2 film during contact-heat cycles. Reproduced with permission from ref. 32. Copyright 2020, Springer Nature. (c) Layout of verifying the dominant role of electron transfer by spin conversion under external magnetic fields. (d) Variation of surface charge density on the Fe_3O_4 film in contacting with O_2-containing DI water under different magnetic conditions. (e) Schematic illustration of promoted charge transfer due to applied magnetic fields. Reproduced with permission from ref. 64. Copyright 2022, Springer Nature. (f) Measured chemiluminescence performance of the potassium ferricyanide when the luminol droplet carries different polarities of charges. (g) Proposed reaction path for explaining the difference in CL. Reproduced with permission from ref. 97. Copyright 2022, American Chemistry Society.

A ferrimagnetic film was first deposited on a highly doped silicon wafer, which was then placed inside a liquid cell with a temperature controller. The magnetic field was provided by an electromagnetic coil beneath it. Exemplified by CE between O_2-containing DI water and Fe_3O_4 in Fig. 3d, the surface charge density could be significantly enhanced by applying a magnetic field (0.5 T), indicating that electrons should be the dominant charge carrier in this scenario. Besides, this magnetic field-induced electron transfer is mostly irreversible since no apparent decrease in charge density was observed even if the magnetic field was removed. A spin-selected electron transfer model is proposed in Fig. 3e for illustrating the magnetic field-promoted CE procedure. HO_2 radicals in the solution and electrons from the 3d orbital of Fe_3O_4 were considered as a radical pair. In the absence of magnetic field, the electron transfer could occur only when the spin of unpaired electrons in HO_2 is antiparallel to that of 3d electrons of Fe_3O_4. The existence of magnetic field could not only align magnetic domains in Fe_3O_4, but also render T–S spin conversion of the radical pair according to the radical pair mechanism.[94–96] Thus, the electron transfer process could be greatly facilitated by applying magnetic fields. The overall magnetic field-promoted electron transfer process could be described as follows.

$$\uparrow O{=}O\uparrow + \downarrow e^{-}(\text{donated by } Fe_3O_4, CoFe_2O_4) + H_2O \Leftrightarrow \uparrow O{=}O\uparrow\downarrow H + OH^{-} \quad (1)$$

$$\uparrow O{=}O\uparrow\downarrow H + \downarrow e^{-}(\text{donated by } Fe_3O_4, CoFe_2O_4) + H_2O \Leftrightarrow H\downarrow\uparrow O{=}O\uparrow\downarrow H + OH^{-} \quad (2)$$

In addition to the KPFM-based study, Zhang *et al.* have verified the dominant role of electron transfer from the aspect of chemical reactions.[97] A luminol droplet was electrified by sliding through a polymer film before it was mixed with potassium ferricyanide aqueous solutions. The polarity of this droplet depended on the CE abilities of polymers. For example, the droplet will be negatively charged if the PTFE film was employed and will be positively charged in the case of nylon films. Results in Fig. 3f suggest that the light intensity and

reaction rate of chemiluminescence (CL) on the potassium ferricyanide could be enhanced by a positively charged droplet, while could be prohibited by a negatively charged droplet. This disparity could be attributed to the electron transfer process during CE between the droplet and corresponding polymer films, as shown in Fig. 3g. To be specific, electrons were transferred from the droplet to the PTFE film, resulting in a positively charged droplet that creates an ordered solvent environment for promoting CL. While under conditions of CE with nylon films, electrons were grabbed by the droplet, which is supposed to hinder the CL process by reducing Fe^{3+} ions to Fe^{2+}.

2.1.3. Wang's hybrid EDL model and its "two-step" formation process. An electric double layer (EDL) spontaneously forms when solids contact with liquids, meanwhile the contact-electrification also occurs at the liquid–solid contact interface.[98–100] Electron transfer occurs and sometimes dominates the charge transfer process of L–S CE,[32,101–103] which implies that there is an impact of electron transfer on the formation of an EDL. A hybrid EDL model that considers both the electron transfer and ion adsorption effects for the formation of an EDL was first proposed by Wang *et al.* in 2018,[38] which is also referred to Wang's hybrid EDL model (Fig. 4). The formation of Wang's hybrid EDL can be specified by a "two-step" process. In the first step, molecules and ions in the liquid will collide with solid surfaces driven by thermal motion or fluid pressure. Electrons will be exchanged at the L–S interfaces due to the overlap of the corresponding electron clouds, and ions will also be adsorbed on the solid surfaces simultaneously. This step explains the origin and composition of initial charges on solid surfaces that remain obscure in the conventional EDL model. The second step is similar to the conventional EDL model that free ions in the liquid are electrostatically attracted to the charged solid surface, forming the EDL.

Wang's hybrid EDL model is compatible with all L–S interfaces since the CE effect and electron transfer driven by it exist ubiquitously.[46] Not to mention that surface defects are common in realistic materials, and these defects are usually trap sites for electrons. Thus, the electron exchange is usually inevitable during the formation of an EDL. Besides, this hybrid model is especially suitable for L–S interfaces where the charge transfer process of CE is dominated by electrons, such as polymer–liquid interfaces.[32] In these cases, the contribution from electron transfer to the formation of EDL is too strong to be ignored. For example, although some ions could be adsorbed on the surface of FEP during its contact with water, the strong electron-withdrawing (EW) ability of groups (such as F atoms) of FEP could directly obtain plenty of electrons from water molecules.[70] The surface of FEP after CE is dominated by electrons instead of ions, which contradicts to the presumption of the conventional EDL model that the solid surface is fully adsorbed with ions. Thus, a more accurate description of the EDL could be derived from the Wang's hybrid EDL model. Moreover, by leveraging the thermionic emission of electrons, the distribution of electrons and ions on the solid surfaces could also be determined using Wang's hybrid EDL model. Exemplified by CE between SiO_2 and water, the calculated distance between two adjacent electrons on the SiO_2 surface is about 16 nm, while that of two adjacent ions is around 30 nm. These distances are much larger than the thickness of the Stern layer, suggesting that a much-finer structure of the EDL could be presented by further considering distances between adjacent charges in Wang's hybrid EDL model.

In summary, Wang's hybrid EDL model provides a more complete theoretical framework for understanding the charge transfer process and formation of EDL at L–S interfaces. For instance, owing to the contribution from electron transfer at the first step of forming an EDL, the structure of the EDL will be significantly affected by the CE ability of solids, which has been neglected in previous investigations of EDLs. Additionally, EDLs also play a vital role in a series of significant application

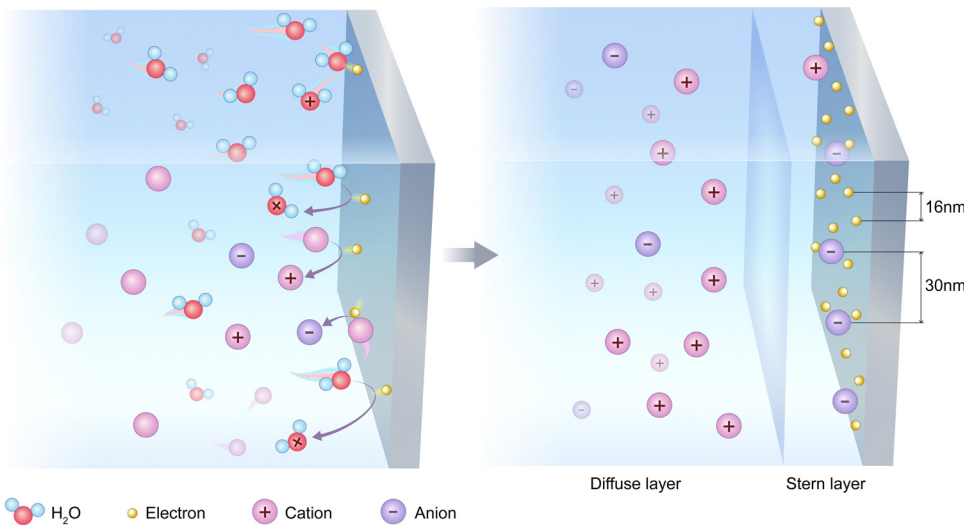

Fig. 4 Wang's hybrid EDL model and its "two-step" formation process. Electron transfer was considered at the first step, and the distribution of electrons as well as ions on the solid surface could be determined (exemplified by SiO_2 contacting water), which is of great significance for understanding the fundamental structure of the EDL.

fields,[104–107] such as heterogeneous catalysis that highly relies on electron/substrate transfer at L–S interfaces.[108–110] Wang's hybrid EDL model is supposed to present better explanations of existing phenomena and may also stimulate the discovery of novel mechanisms in research frontiers.

2.2. From CE-driven electron transfer to contact-electro-catalysis

A typical catalytic process usually consists of three key steps: adsorption, reaction, and desorption.[15,111,112] The reaction step refers to rearrangement of electrons with the assistance of catalysts to produce products, and the driving force for electron transfer or excitation is one of the fundamental differences among various catalytic principles. For instance, the electrons for reaction were exchanged on a charged electrode in electrocatalysis,[113–115] and the electron–hole pairs were excited by light irradiation in photocatalysis.[116–118] Recent studies have verified the existence of electron transfer during contact-electrification (CE),[37,38] and it appears to be the dominant charge transfer mechanism for CE in a majority of cases.[34,83] Prof. Zhong Lin Wang has proposed an electron-cloud-potential-well model to elucidate a generalized scenario of contact-electrification between two materials.[38] As two materials are brought into contact by external mechanical agitations, electron clouds of atoms belonging to these two materials are supposed to overlap, which could lower the energy barrier between these two atoms. Electrons will be transferred from one atom to another once the input energy is sufficient to overcome the energy barrier, and the transferred electron will remain on the other atom, implying that catalyzing the chemical reactions by CE-driven electron exchange should also be feasible.

Furthermore, the charged surface due to CE will create an electric field in space, and a high-intensity electric field is able to significantly affect the ambient environment.[40,41] For example, the electric field can induce polarization or modulate the electronic structure of adjacent molecules, thus changing their chemical activities.[119,120] Moreover, the electric field at contact interfaces can drive the transport and diffusion of charged species, such as electrons.[121,122] Recent studies have suggested that the high-intensity electric field on the surface of water microdroplets is the driving force for electron transfer and subsequent formation of H_2O_2 in sprayed water.[43,123,124] This electric field also exists at water–oil contact interfaces, and the derived electron transfer can catalyze the generation of reactive oxygen species (ROS) for degrading hexadecane.[42] Further investigations have proved that an intensified electric field at interfaces could lead to an accelerated reaction rate by facilitating electron transfer.[44] These experimental observations further support that chemical reactions could be promoted by CE.

Contact-electro-catalysis (CEC), bridging contact-electrification and mechanochemistry, has been proposed as a significant supplement to existing catalytic strategies.[45] The definition of CEC refers to a catalytic process that employs electrons exchanged during contact electrification to promote the rate of chemical reactions. Fig. 5a shows a typical CEC process for redox reactions: Reactant ''A'' first contacts with the CEC catalyst ''C'', and electrons are supposed to be transferred from ''A'' to ''C'' driven by CE. ''A'' will be oxidized to A_{oxd}'' by such electron exchange, and the symbol ''C*'' is proposed to denote the charged state of ''C''. After the desorption of ''A_{oxd}'', the electrons left on the surface of ''C*'' could be obtained by another reactant ''B'' upon their contact. ''B'' will be reduced to ''B_{red}'', and ''C*'' will retrieve its initial uncharged state ''C'', completing an entire catalytic cycle. Exemplified by the CE-driven electron transfer between the FEP particles and the surrounding substrates, a detailed CEC process for producing ROS could be expressed as shown in Fig. 5b. According to the triboelectric series, electrons will be exchanged to FEP upon their contact with water molecules.[46,70,73] After losing electrons, water molecules are first converted to water radical cations, followed by the production of hydronium cations and hydroxyl radicals through a rapid proton transfer.[125–127] The term FEP* is introduced to represent the charged state of FEP. Electrons from the surface of FEP* are captured by O_2 molecules when they collide with FEP*, resulting in the formation of superoxide radicals and the restoration of FEP to its original uncharged state. This cycle will continue as long as the mechanical stimuli persist.

2.3. Broad catalysts enabled by CEC

Contact-electrification is widely existed at various surfaces, such as interfaces for solid–solid,[59,63,128] solid–liquid,[60,129,130] and even liquid–liquid[61,67,68] or solid–gas contact.[131] The ubiquity of CE endows the CE-based CEC with a much broader array of catalyst options (Fig. 6). On the one hand, the CE could take place at both micro- and macro- scales,[35,53,83] which minimizes restrictions for the configuration of CEC catalysts. For instance, powders at the micrometer scale,[45,48,49] millimeter-sized spheres, and even centimeter-scale films have all been demonstrated as viable candidates for CEC catalysts.[50] On the other hand, the operating principle of CEC refers to promote chemical reactions by CE-driven interfacial electron exchange, which is majorly dependent on the surface properties of the employed materials. Thus, the category of CEC catalysts could be considerably diversified that can be divided into three types in general: polymers, oxides, and matrix composites. We expect the combination of various configurations and categories of CEC catalysts could provide plenty of room for designing catalytic systems towards a more sustainable and efficient way.

Pristine polymers, due to their outstanding contact-electrification (CE) capabilities and inherent catalytic inertness, were the first reported CEC catalysts.[45] Their successful application also provides compelling evidence for the feasibility of CEC. Specifically, Wang *et al.* have proved that CEC is the dominant mechanism for catalytic degradation of methyl orange (MO) aqueous solution during ultrasonication in the presence of fluorinated ethylene propylene (FEP) powder.[45] This degradation is effective even when FEP was replaced by other pristine polymers such as polytetrafluoroethylene (PTFE), rubber, and nylon, as long as they exhibited satisfying CE abilities. The dominant role of CEC was further confirmed by the fact that received catalytic efficiency aligns well with the CE ability of these polymers. Besides, we expect that a Janus-structured

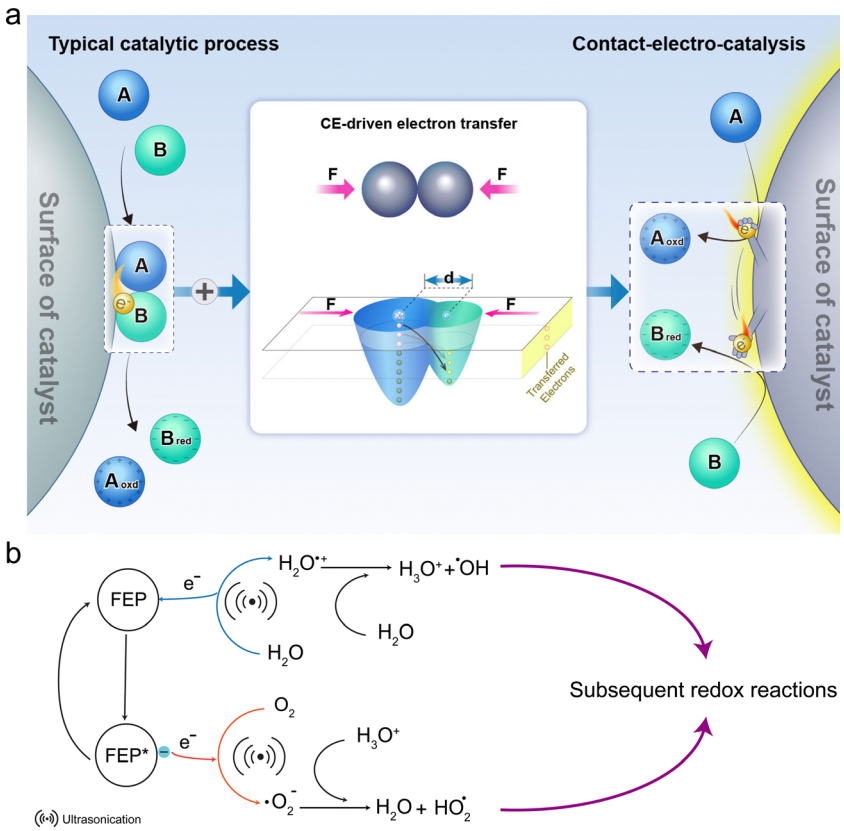

Fig. 5 From CE-driven electron transfer to contact-electro-catalysis. (a) Contact-electro-catalysis (CEC) was proposed by using the CE effect to drive electron transfer in a typical catalytic process, where the ''grab'' from and ''release'' of an electron from water molecule is animated. (b) A specific CEC process for producing ROS by ultrasonication in the presence of FEP.

polymer that incorporates a metal layer at the backside could significantly improve the efficiency of polymer-based CEC. The enhancement might be explained by the concept of ''mirror charge''. The charged surface of the polymer could supply a high-intensity electric field to polarize adjacent metals, which renders the outer surface of metals also being charged. Different from the ''bounded state'' of electrons on polymer surfaces, induced electrons on metal surfaces are readily exchanged to other substrates for catalyzing the generation of reactive oxygen species (ROS). Hence, the yield of ROS could be significantly promoted by using polymer–metal Janus composites in CEC. In addition, we envision that the concept of ''mirror charge'' may also be feasible for improving the efficiency of existing metal-based catalysts *via* a conventional route since the CE effect appears ubiquitously among various interfaces.

Unfortunately, however, the decreased CE ability of polymers due to glass transition at elevated temperature may impede the application of CEC in catalyzing chemical reactions that usually occur at high temperatures.[37,132] To address this limitation, oxide-based CEC was proposed by Li *et al.* that employs SiO_2 to withstand the high temperature required for recycling cathode materials in spent lithium-ion batteries (LIBs).[54] The leaching efficiency in the SiO_2 group is around 10% higher than that in the PTFE group when temperature was set to 70 °C. Although SiO_2 is applicable for high temperature conditions, its intrinsic poor CE performance renders a relatively sluggish reaction rate. Chen *et al.* have introduced a fluorinated layer on SiO_2 to enhance its CE ability and corresponding CEC efficiency.[133] The MO aqueous solution could be effectively degraded by fluorinated SiO_2 in 3 h, while no apparent discoloration of MO was observed in the control group without a fluorinated layer. More importantly, a Fe_3O_4 core was also designed inside the fluorinated SiO_2, which could greatly facilitate the recovery of CEC catalysts through the magnetic properties of Fe_3O_4. In addition to inorganic non-metallic oxides, metal oxides such as TiO_2 were also explored for CEC by using the tribovoltaic effect. Lin *et al.* have added TiO_2 as well as Al particles into an organic dye solution and employed ultrasonication or stirring to induce collisions between these particles.[134] Electron–hole (e–h) pairs are supposed to be excited at the dynamic contact interfaces of TiO_2 and Al due to the tribovoltaic effect,[135–137] which could in turn catalyze the generation of ROS to degrade target organic pollutants.

The diversity of CEC catalysts also provides abundant opportunities for collaboration with existing catalytic strategies. Metal–organic frameworks (MOFs) have emerged as a promising category of heterogeneous catalysts that generally employ transition metal centres to provide active sites for catalysis.[138–140] A possible strategy for incorporating CEC with

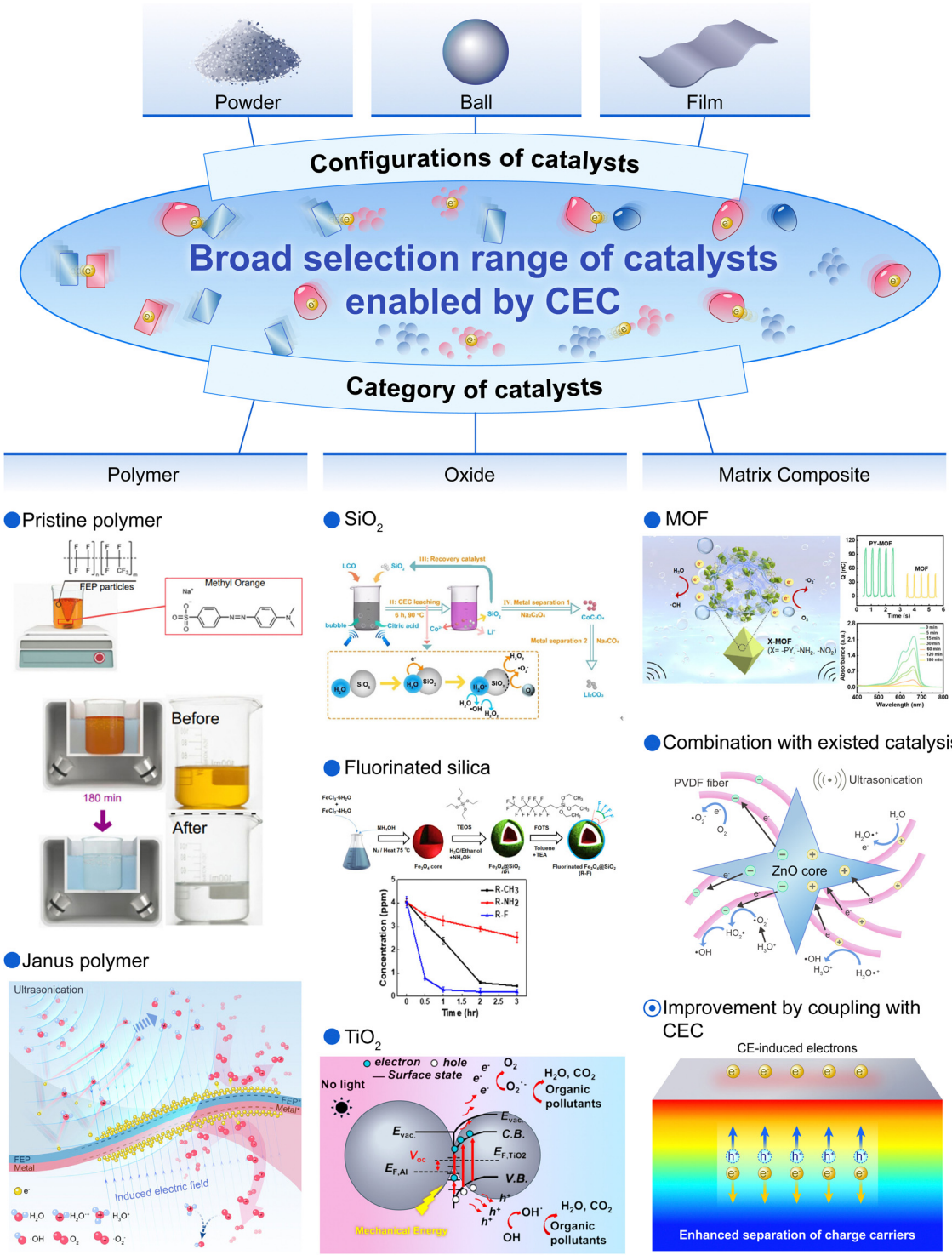

Fig. 6 CEC-expanded selection range of materials that can be envisaged as catalysts. Various materials have been proposed for the CEC process with diverse configurations and categories. Meanwhile, a synergistic effect between CEC and existing catalytic strategies is expected for a much-improved efficiency. Reproduced with permission from ref. 45,54,133,134,141,142. Copyright 2022, Springer Nature and Elsevier.

a MOF was proposed by Zhang *et al.* that has grafted pyridine molecular groups on the surface of pristine MIL-101(Cr) to enhance its CE performance.[141] The modified MOF could effectively degrade methylene blue through CEC. Integration of CEC with piezocatalysis was also demonstrated by Jiang *et al.* where ZnO cores were surrounded by PVDF fibers through electrospinning.[142] A 444.23% higher degradation rate was achieved by the prepared ZnO@PVDF composite when compared to the pure PVDF membrane. In addition to direct combination with CEC, we also expect a much-improved

catalytic efficiency *via* synergistic effects between the CE and existing catalytic mechanisms. For instance, we assume that appropriate surface modifications could enhance the CE abilities of conventional catalysts without obvious sacrifice of their original catalytic activity. CE-induced electrons on the surface could not only directly participate in chemical reactions to boost the reaction rate, but may also provide a high-intensity local electric-field to facilitate the separation of charge carriers in conventional catalysts. Thus, the catalytic efficiency is supposed to be significantly improved by coupling CEC with existing catalytic strategies.

2.4. Strategies for initiating CEC

The essence for initiating contact-electro-catalysis relies on introducing effective contact-separation cycles on target interfaces. Electron exchanges during such cycles are supposed to promote the rate of chemical reactions. Fig. 7 presents representative strategies for initiating CEC. Ultrasonication was first proposed for inducing CEC, which utilizes the variation of cavitation bubbles during the propagation of ultrasonic waves.[45] Specifically, nuclei of cavitation bubbles tend to form near dissolved gases (O_2, for example) and the growth of nuclei will enclose these adjacent gas molecules. Once a cavitation bubble surpasses a critical size, its implosion will release contained gas molecules, producing a high pressure microjet that could cause contact-separation cycles and the corresponding electron exchange. Reactive oxygen species (ROS) including hydroxyl and superoxide radicals can be produced by FEP particles in the presence of ultrasonication, and these ROS were effective for degradation of organic pollutants or direct synthesis of H_2O_2.[48] Besides, Wang *et al.* have found that ultrasonication could not only induce high-frequency CE, but also provide a high-pressure environment to facilitate the generation of ROS by decreasing the energy barrier for electron transfer.[45]

Ball milling is another representative strategy for initiating CEC, which could naturally bring about frequent contacts and separations.[143] The presence of triboelectric materials is expected to induce an apparent CE phenomenon during such collisions, implying that the CEC could be realized by using triboelectric materials in ball milling. Wang *et al.* have examined the feasibility through a liquid-assisted grinding (LAG) setup that is made of triboelectric materials. A series of parallel experiments were conducted under identical conditions, except

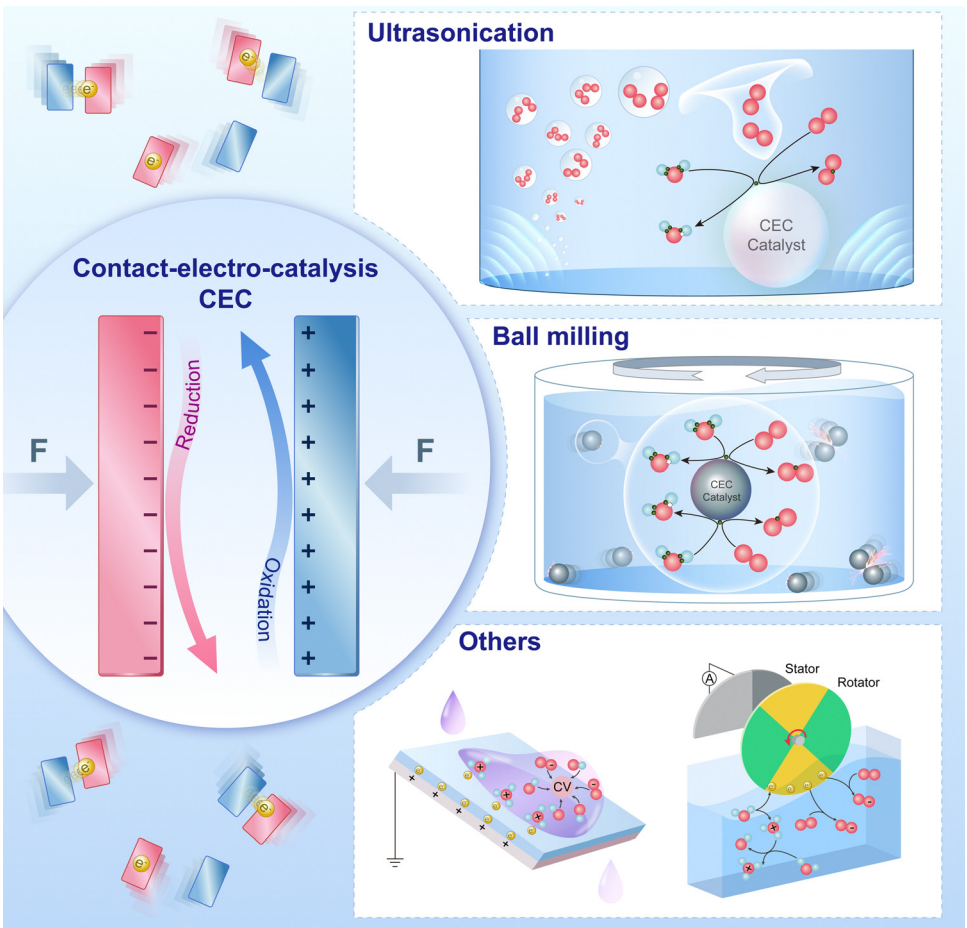

Fig. 7 Strategies for initiating the contact-electro-catalysis. To date, ultrasonication and ball milling have been two representative approaches used for effectively initiating CEC. Besides, contributions from physical adsorption that arises from electrostatic attraction by a charged solid surface were appropriately recognized in all reported methods. Reproduced with permission from ref. 45,143–145. Copyright 2022, Springer Nature and Elsevier.

different triboelectric materials being employed. ROS could be catalytically produced through CE-driven electron transfer, and the received concentrations correlate with the CE ability of utilized materials. The dominant role of CEC was further revealed by a control experiment that uses a conventional ZrO_2 ball mill setup. Although ZrO_2 is supposed to provide a higher energy impact during grinding, the catalytic efficiency is still much lower than that in the PTFE group. This result also suggests that the high energy impact is not necessary for CEC to take place, which is beneficial for improving the recyclability and reusability of catalysts. We speculate that developing materials with higher CE ability may initiate CEC under an even milder condition. Meanwhile, ball milling also provides an ideal platform to investigate the relationship between CE and CEC. Despite that CE could occur at any revolution speeds, there exists a speed threshold for initiating CEC. This interesting phenomenon stimulates us to explore the underlying mechanism and one possible reason should be that the energy of exchanged electrons during CE is insufficient when the revolution speed is low. A further increase in revolution speeds will result in an enhanced rate for producing ROS, which can be explained by the improvement of impact frequency and decreased energy barrier for interfacial electron transfer at elevated revolution speeds.

Other strategies including a droplet sliding through a polymer surface and immersing a triboelectric nanogenerator (TENG) into aqueous solution have also been reported.[144,145] These approaches require utilizing facile and intuitive contact-separation at liquid–solid interfaces, and the discoloration of dye solutions is very effective. However, we should be aware that physical adsorption might play a dominant role in discoloration. The polarity of target dye ions is reversed to that of employed materials in these cases. For example, crystal violet (CV) is a cationic dye and the surface of FEP is negatively charged after CE with water. Thus, the positively charged CV molecules could be electrostatically adsorbed on negatively charged FEP surfaces, and this kind of adsorption is assumed to hinder further CE on FEP, resulting in the ''choke of catalysts''. To improve the contribution from chemical degradation, efforts should focus on improving the frequency of CE or supplying higher energy for overcoming the energy barrier for CE-driven electron exchange.

2.5. Two-step mechanism of CEC

A two-step model for producing ROS by CEC was first proposed by Wang *et al.*, and involves the oxidation of water and reduction of oxygen molecules as explicated using eqn (3) and (4).[45] In the first step, electrons will be transferred from water molecules to FEP upon their contact. Water radical cations were formed due to such electron transfer, and they will undergo a rapid proton transfer with another water molecule for producing hydronium cations and hydroxyl radicals.[125–127] FEP* was employed to describe the status of FEP after obtaining electrons from water molecules. In the second step, electrons on FEP* will be exchanged to the oxygen molecules when dissolved oxygen in aqueous solutions comes into contact with FEP*, forming superoxide radicals. In the meantime, FEP will retrieve its initial uncharged state, completing an entire cycle.

$$2H_2O + FEP \rightarrow H_3O^+ + OH^\bullet + FEP^*. \quad (3)$$

$$O_2 + FEP^* \rightarrow {}^\bullet O_2^- + FEP. \quad (4)$$

In eqn (3), H_2O first loses one electron and becomes H_2O^+, but the life time of H_2O^+ is less than 200 ps, which immediately combines with another H_2O molecule, leading to

$$H_2O + H_2O^+ \rightarrow H_3O^+ + OH^\bullet \quad (5)$$

ab initio molecular dynamic calculations suggest that the hydrogen bond network of water could facilitate the exchange of protons and electrons during CEC.[49]

Zhao *et al.* have performed a detailed study on the two-step mechanism for producing ROS by CEC as demonstrated in Fig. 8a.[146] A DI water droplet was injected into a PTFE-made capillary tube, and then pushed by N_2 gases to pass through the tube. A control group was conducted under the same conditions except that the tube was subjected to ultrasonication. Droplets at the end of both tubes were collected for further characterization. Electron paramagnetic resonance (EPR) results in Fig. 8b indicate that the use of ultrasonication could promote the generation of hydroxyl radicals, while superoxide radicals are exclusively produced in the presence of ultrasonication. The facilitation of producing hydroxyl radicals could be ascribed to that the ultrasonication not only provides additional chances for CE, but also offers extra energy for CE-driven electron transfer. The underlying mechanism for the difference in producing hydroxyl and superoxide radicals might be that the PTFE inclines to obtain electrons, which renders the process of PTFE grabbing electrons from H_2O molecules to produce hydroxyl radicals is energy efficient.[70] Thus, the generation of hydroxyl radicals could be catalyzed directly by CE between droplets and the inner wall of PTFE tubes. However, in the case of producing superoxide radicals, electrons need to be removed from the electron-affinitive surface of PTFE, resulting in a much higher energy for accomplishing this process. Density functional theory (DFT) calculations for the positions of LUMO and HOMO for H_2O-PTFE and O_2-PTFE have confirmed the assumption, as shown in Fig. 8c[48] Owing to the weak-coupling limit, the difference between the LUMO of the acceptor and the HOMO of the donor is considered as equivalent to the energy barrier for charge transfer.[45] Nearly 1 eV more energy is required for transferring electrons from charged PTFE (PTFE*) to O_2 molecules, indicating that the process of producing superoxide radicals should be the rate determining step. This high energy barrier could be overcome by improving the energy input, such as using ultrasonication. Not to mention that the high- pressure environment during ultrasonication could further reduce the energy barrier for electron exchanging.

Taking PTFE as an example, a more complete two-step mechanism for generating ROS through CEC is described in Fig. 8d. At the first step, electrons will be transferred from H_2O to PTFE upon their contact, producing water radical cations that would be converted to hydronium cations and hydroxyl

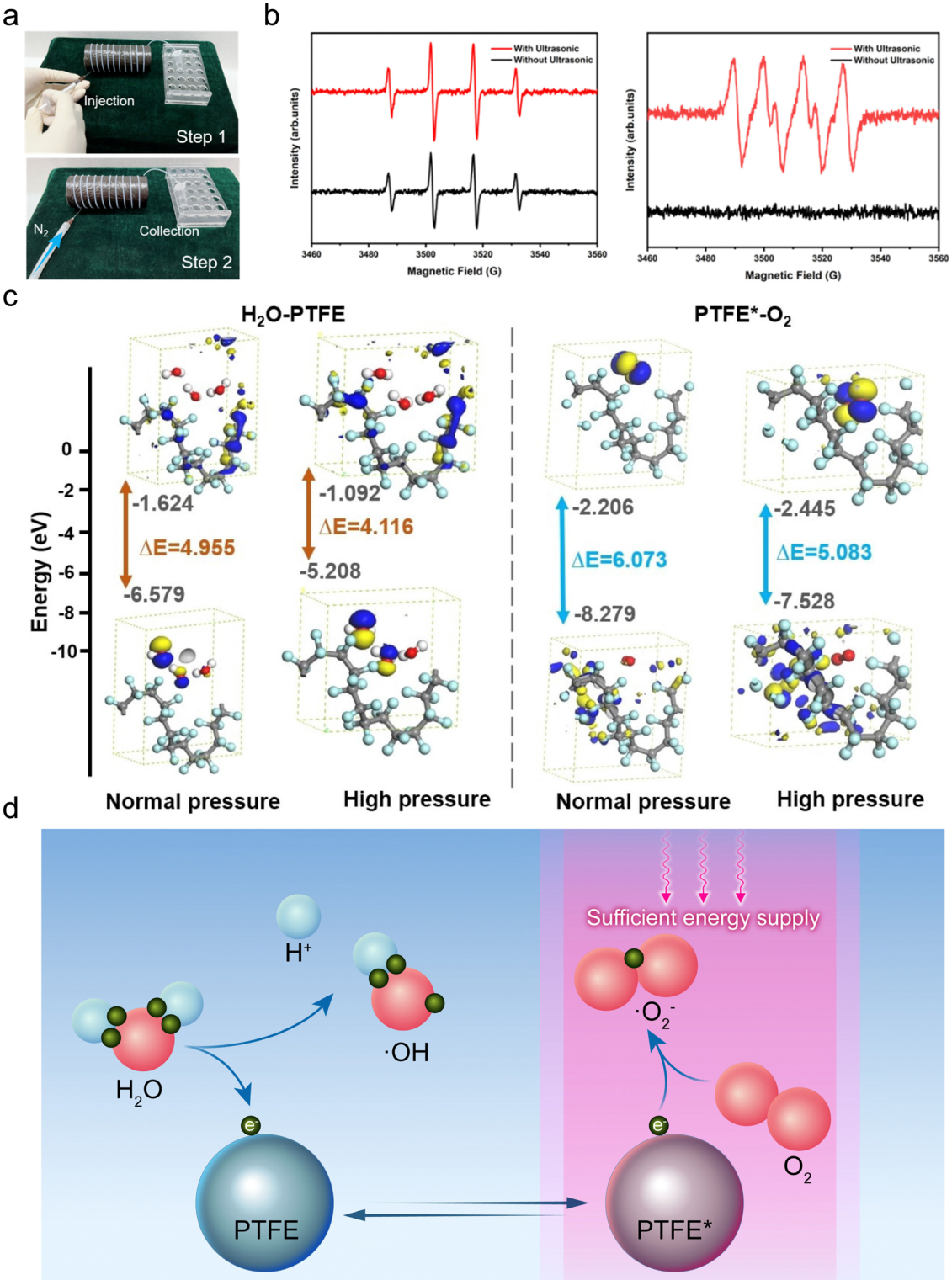

Fig. 8 Two-step mechanism for generating ROS through CEC. (a) Optical images illustrating the process of CEC. (b) Measured EPR profiles under conditions of with and without ultrasonication. Reproduced with permission from ref. 146. Copyright 2022, Elsevier. (c) DFT calculations of the values of LUMO and HOMO levels for H_2O-PTFE and O_2-PTFE under various conditions. Reproduced with permission from ref. 48. Copyright 2022, Wiley. (d) Proposed two-step mechanism for producing radical oxygen species through CEC.

radicals through a rapid proton transfer from water. Electrons accumulated on the charged surface of PTFE* will be exchanged to dissolved O_2 molecules once they collide with adequate energy, which is denoted as the second step. PTFE* will retrieve its initial uncharged states, and O_2 will be converted to superoxide radicals after obtaining these electrons.

This cycle repeats itself as long as the mechanical stimuli are sustained.

2.6. Factors influencing CEC

In the pursuit of a better understanding of the underlying principle and optimization of CEC efficiency, investigations into factors influencing CEC were also carried out.[132] Because ultrasonic frequency and power could significantly affect the size and quantity of cavitation bubbles that are regarded as the source of contact-separation cycles, Dong *et al.* have developed a frequency- and power-adjustable ultrasonic reactor to examine the correlation between the CEC efficiency and these parameters. Taking degradation of methyl orange aqueous solution as a model reaction, Fig. 9a suggests that a higher degradation rate was obtained with the increment of ultrasonic power when the frequency was fixed at 40 kHz. This tendency could be attributed to enhanced CE frequencies because more cavitation bubbles will be generated by increased ultrasonic power.[147] However, a larger number of smaller size cavitation bubbles were expected as the ultrasonic frequency increases under the same power.[148] Although the CE frequency could be promoted by enhanced quantity of cavitation bubbles, the implosion of smaller cavitation bubbles is supposed to release less energy that will be utilised in the CE-driven electron transfer. Therefore, the efficiency of CEC is supposed to increase with the rise of ultrasonic frequencies at the initial stage, and then decreased due to insufficient energy for driving electron transfer. The obtained results shown in Fig. 9b concur with the assumption that the optimum frequency was 40 kHz. Temperature is another vital parameter that would not only directly influence the reaction rate through activation energy, but also affect the physical nature of polymers and stability of electrons on the surface. Fig. 9c indicates that the optimum temperature for CEC was between 20 and 30 °C, which could be ascribed to the fact that the glass transition of polymers would affect their CE performance, and such a transition usually takes place from a temperature as low as 15 °C. Developing materials that are capable of exhibiting robust CE performance even at elevated temperatures holds promise for further enhancement of CEC efficiency.

Revolution speed is a crucial parameter that could greatly change the impact mode/energy of ball milling.[149] Thus, the optimum conditions for CEC in ball milling were examined from the aspect of revolution speeds.[150] Degrading MO was also regarded as the model reaction, and the evolution of MO relative concentrations under different revolution speeds is shown in Fig. 9d.[143] Almost no degradation was observed when the revolution speed is lower than 100 rpm. However, a 19.5-times higher degradation rate was observed once the revolution speed was increased to 150 rpm, and the degradation rate rises at elevated revolution speeds. Given that both collision frequency and impact energy are related to revolution speeds, a control experiment was carried out at a low revolution speed (50 rpm) with a prolonged milling time (600 min) to explore the

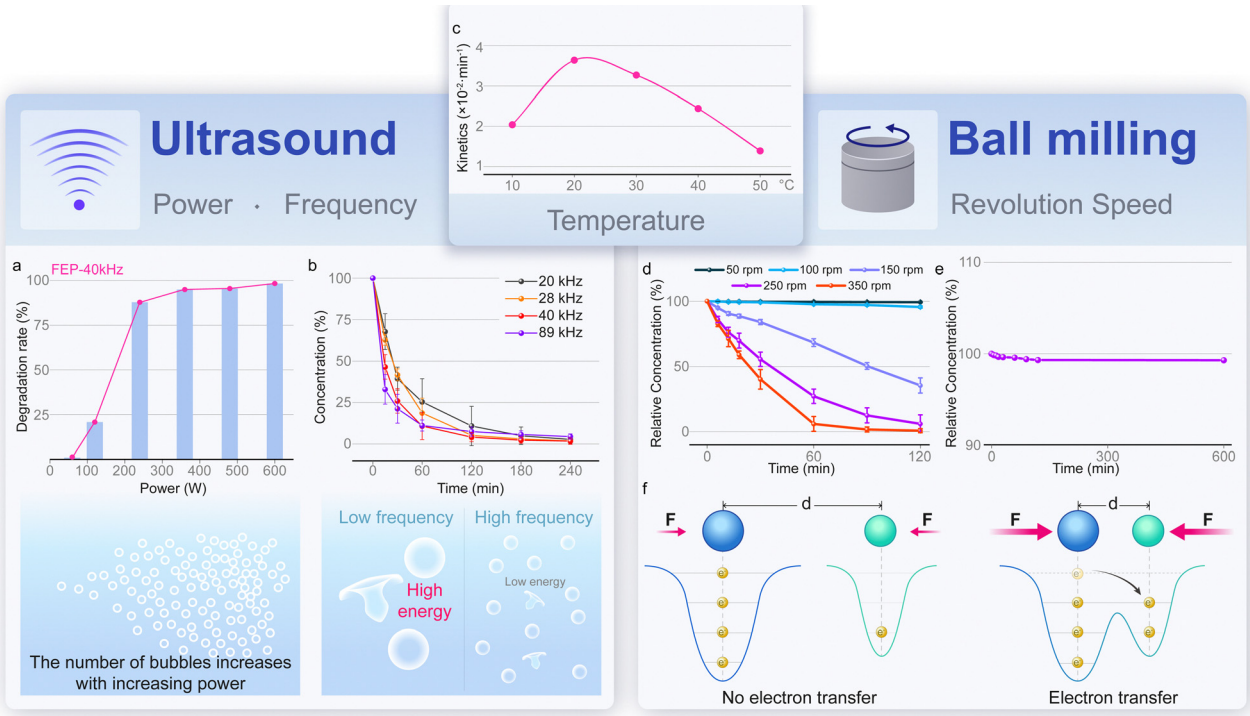

Fig. 9 Factors influencing contact-electro-catalysis. (a) Degradation rate of MO under various ultrasonic powers with a fixed frequency at 40 kHz. (b) Evolution of MO under conditions of various ultrasonic frequencies and a fixed power of 600 W. (c) Correlation between the temperature and kinetics of degrading MO during ultrasonication. Reproduced with permission from ref. 132. Copyright 2022, Elsevier. (d) Evolution of MO absorbance under different revolution speeds of ball milling. (e) Degradation rate of MO under 50 rpm for 600 min. (f) Proposed mechanism for illustrating the existence of speed threshold for initiating CEC in ball milling. Reproduced with permission from ref. 143. Copyright 2022, Springer Nature.

dominant mechanism. Measured variation of the MO relative concentration in Fig. 9e suggests that the low collision frequency is not the major reason for poor CEC efficiency at low revolution speeds. A better explanation was proposed from the impact energy and its effect in CE, as depicted by an electron-cloud-potential-well model shown in Fig. 9f. The corresponding overlapping of electron clouds at the atomic scale is expected when two interfaces are brought into contact through external force. A higher applied force is supposed to result in a more pronounced overlap of electron clouds which is beneficial for facilitating electron transfer between the corresponding atoms. Thus, there might exist a speed threshold, below which the impact energy is insufficient to overcome the energy barrier for electron transfer. Once the speed becomes beyond this critical value, not only the impact energy is enhanced, but also the energy barrier is reduced, giving rise to a much higher quantity of transferred electrons for facilitating the CEC. Not to mention that the frequency of CE will also increase due to enhanced collision frequency at elevated revolution speeds.

3. Significant applications of contact-electro-catalysis

3.1. Organic pollutant degradation

Organic wastewater originates from a wide range of sources, such as chemical manufacturing, food processing, industrial facilities (point source), and also diffused pesticides or fertilizers during agricultural runoff (non-point source).[151,152] Degrading organic pollutants in water resources is of paramount importance due to its significant impact on both the environment and human health.[153,154] The application of CEC in degrading organic pollutants in water resources possesses several unique advantages, as depicted in Fig. 10. On the one hand, since almost no restriction is existed for a material to operate as a catalyst for CEC, not only the selection range for catalysts has been much expanded, but also the process for synthesizing catalysts has been greatly simplified. Even natural materials such as rocks can potentially be catalysts for CEC. On the other hand, the energy source for CEC is mechanical stimuli such as vibrations, sliding, collision, grinding and ultrasonication, which are readily available in an ambient environment though usually be ignored. Hence, the degradation of organic pollutants by CEC can take place even in remote wilderness areas that are far away from electricity, lights, and synthetic materials, potentially shedding light on the phenomenon of running water does not rot. Besides, owing to the shape of catalysts could be powders, balls, or even films, and no harsh conditions are involved during the reaction, the CEC catalysts could be effectively recycled by simple filtration, and collected CEC catalysts are supposed to exhibit excellent recyclability and reusability. For example, almost no diminution in catalytic efficiency was observed after FEP particles being reused 5 times.[45]

Methyl orange (MO) aqueous solution, a typical refractory and mutagenic organic compound, can be effectively degraded in the presence of FEP powder *via* ultrasonication. In addition to ultrasonication, ball milling has also been proved as an effective strategy to degrade organic pollutants through CEC, and its efficiency is even higher than that of ultrasonication. Moreover, other organic pollutants such as acid orange 17 (AO-17) and rhodamine B (RhB) could also be decolored. However, we should notice that the mechanism for discoloration of RhB is different from that for other two dyes. RhB is a cationic dye that is supposed to be electrostatically adsorbed on the negatively charged surface of FEP, and CE at the adsorption site will be prohibited by these dye molecules. Thus, physical adsorption instead of chemical degradation plays a dominant role in discoloration of RhB. A wastewater treatment system was also devised to fully exploit the advantages of CEC. Dielectric powders were first dispersed in wastewater using a homogenizer, followed by transferring the prepared suspension to an ultrasonic reactor for purification. Purified water could be directly released and dielectric powders in it could be facilely separated using a filtration system. Separated powders could be recycled and reused for the next purification cycle.

3.2. Direct synthesis of H_2O_2

Hydrogen peroxide is a versatile chemical compound with a broad range of applications in chemical synthesis, environmental remediation, and the electronics industry.[155–158] However, the formation of hydrogen peroxide is thermodynamically unfavorable and involves multiple reaction steps as well as intermediate species, which renders the preparation of H_2O_2 rather challenging especially under ambient conditions.[159–161] CEC has emerged as a promising candidate for properly addressing these difficulties due to its salient features of cost-effectiveness, environmental friendliness, and scalability. First of all, the conditions for producing H_2O_2 through CEC are inexpensive ultrasonication and using commercially available PTFE particles at room temperature, which not only avoid the use of noble metal catalysts such as palladium, but also reduce energy consumption since neither high-pressure nor high-temperature conditions are required. Besides, no hazardous reactants are employed as well as no environmentally harmful intermediates or side products will be formed during the reaction, which enable the entire process sustainable with minimized environmental impact. More importantly, the production of H_2O_2 by CEC could be easily and safely scaled up since every particle dispersed in the solution could act as reaction sites and no danger of H_2 explosion exists, further highlighting the practicability of preparing H_2O_2 by CEC.

Zhao *et al.* have reported a facile strategy for direct synthesis of H_2O_2 under ambient or even anaerobic conditions through CEC, and a detailed mechanistic study was conducted by Berbille *et al.*, as shown in Fig. 11.[48,49] PTFE particles were dispersed into DI water and ultrasonication was employed to initiate CEC. PTFE particles will be separated using a nanoporous membrane, and produced H_2O_2 can be collected at the product chamber for further applications. Isotope labelling experiment coupled with LC-MS analysis have been conducted to reveal the catalytic mechanism of producing H_2O_2. Similar to the mechanism for generating ROS by CEC, the water oxidation

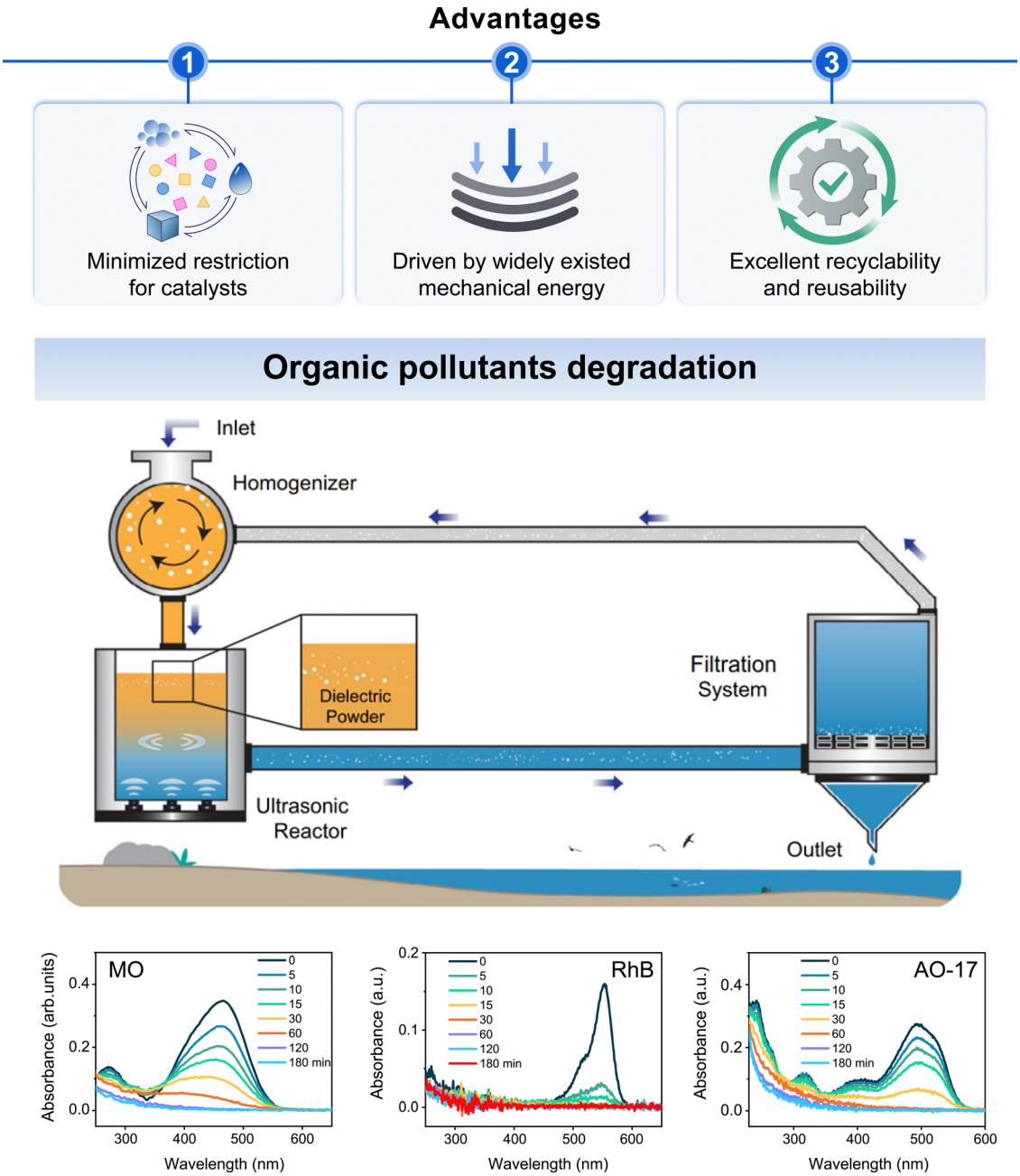

Fig. 10 Significant application of CEC: organic pollutant degradation. Several representative organic pollutants could all be effectively degraded by CEC, and catalysts in CEC demonstrate excellent recyclability and reusability. Meanwhile, such a process could naturally happen in the environment, which might be the potential mechanism illustrating why the running water does not rot. Reproduced with permission from ref. 45. Copyright 2022, Springer Nature.

reaction (WOR) and the oxygen reduction reaction (ORR) could both contribute to the formation of H_2O_2 by CEC. In the WOR path, a water molecule loses an electron to PTFE particles that would produce a hydroxy radical. The recombination of two hydroxy radicals will give rise to a hydrogen peroxide molecule. Oxygen is not necessary for producing H_2O_2 *via* this path, indicating the synthesis of H_2O_2 *via* CEC could be achieved under anaerobic conditions. For the ORR path, oxygen molecules will attain electrons from the charged surface of PTFE, forming superoxide radicals. Produced superoxide radicals will first protonate to hydroperoxyl radicals ($^{\bullet}OOH$), and then simultaneously obtain a proton and an electron for conversion to hydrogen peroxide. The WOR should be the dominant reaction path for yielding H_2O_2 not only because this path requires less energy to take place, but also the ORR path needs to compete with a $4e^-$-ORR side reaction that leads to the formation of water molecules. Moreover, *ab initio* molecular dynamics calculations suggest that the hydrogen bond network of water could facilitate the exchange of protons and electrons for producing H_2O_2 through CEC.

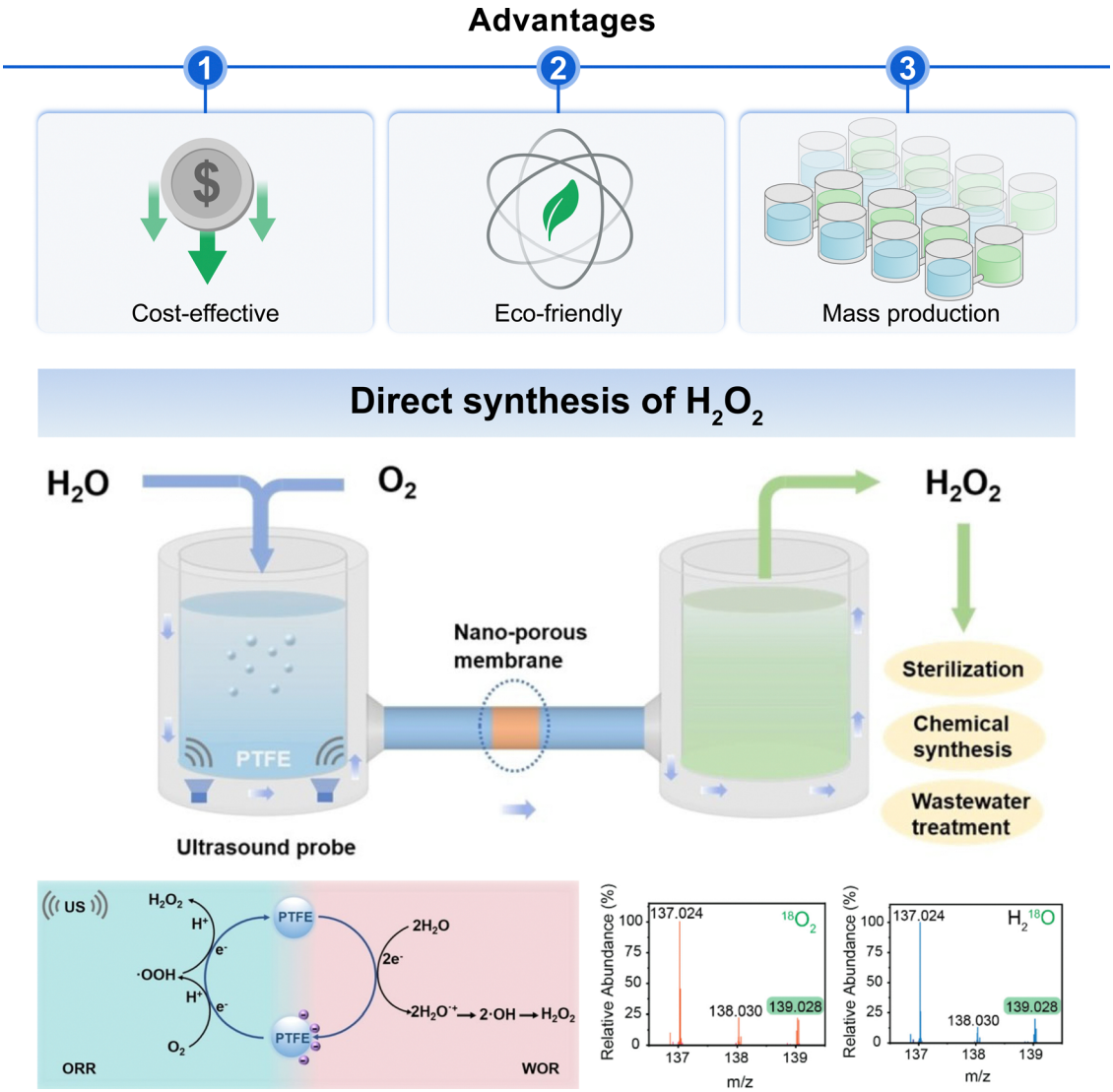

Fig. 11 Significant applications of CEC: direct synthesis of H_2O_2. CEC is a cost-effective and eco-friendly strategy for synthesis of H_2O_2 and even for its mass production. Water oxidation reaction (WOR) and oxygen reduction reaction (ORR) paths have been identified as the underlying mechanism. Reproduced with permission from ref. 48. Copyright 2022, Wiley.

3.3. Recycling of spent lithium-ion batteries

The increasing demand for better lithium-ion batteries (LIBs) has propelled extensive research into the development of advanced electrode materials,[162–164] electrolytes or membranes for achieving higher capacity,[165] faster charge velocity, and elongated cycle life.[166] In addition to these achievements in improving the performance of LIBs, equal attention should be paid to addressing the issue of how to effectively handle spent LIBs.[167] The CEC has provided an efficient and sustainable approach for extracting valuable Li and Co metals from cathode materials in spent LIBs under mild conditions. Distinguished from pyrometallurgy that often performed at a temperature reaching 1400 °C,[168] the recycling of Li and Co metals by CEC can be achieved by ultrasonicating SiO_2 particles in the presence of citric acid at 90 °C. Moreover, citric acid instead of hazardous and expensive strong inorganic acid was employed for CEC, which greatly relieves the damage to environment and simplifies the process of waste management since less wastewater and toxic gases would be produced.[169–171] Although cheap and unconventional SiO_2 particles were used as catalysts, a high leaching efficiency of 100% for Li as well as 92.19% for Co were achieved for lithium cobalt(III) oxide (LCO) batteries, and used SiO_2 could be easily recycled with nearly no diminution in catalytic efficiency.

The detailed procedure for recycling spent LIBs by CEC was proposed by Li *et al.* as demonstrated in Fig. 12. Before mixing with citric acid and SiO_2 particles, the LCO precursor was acquired by disassembling spent LIBs. The obtained suspension was ultrasonicated for 6 h at 90 °C until the solution turns pink. SiO_2 particles were separated by filtration for the next cycle of leaching, and $Na_2C_2O_4$ as well as Na_2CO_3 are added in sequence to residual solution for converting Co^{2+} and Li^+ to CoC_2O_4 and Li_2CO_3, respectively. The principle of leaching can be described as using CE-driven electron transfer on SiO_2

surfaces to produce hydroxyl and superoxide radicals. These radicals in addition with CE-produced electrons could all likely contribute to the leaching of Co^{2+} and Li^{+} ions. As an essential section for evaluating the practicability of the proposed recycle strategy, economic analysis was also conducted, and a profit of \$8.986 per kg spent $LiCoO_2$ powders was achieved, which manifests the superior performance of CEC compared to that of other acid leaching methods. We believe that the feasibility of the CEC strategy could be further improved by subsequent investigations into enhancing the CE ability on SiO_2 surfaces and devising a simpler approach for recycling used catalysts.

3.4. Other promising applications of CEC

ROS has been proved effective for cancer therapy through a series of biochemical effects such as activating immunogenic cell death (ICD) in tumor cells or improving the body's adaptive immune response.[172–174] The primary resources for generating ROS by CEC are water and dissolved oxygen that are ubiquitous in the body, eliminating the requirement of additional chemical reagents. More importantly, the ROS could be *in situ* produced in target positions under external mechanical stimuli (ultrasonication for example). Thus, we believe that the CEC represents a highly controllable and safe strategy for effective anti-cancer treatments. Another promising application field of CEC should be the promotion of solid–solid reactions. The CE effect and the derived electron transfer process also exist at the solid–solid interface. Not to mention that the CE at the solid–solid interface is far more obvious than that at the liquid–solid interface.[70] Hence, in addition to the CEC at L–S interfaces, we suppose that the CEC also holds the promise to catalyze solid–solid reactions which is also one of the unique merits of mechanochemistry.

In addition to these promising applications fields, we should also be aware of that the CEC is currently unsuitable

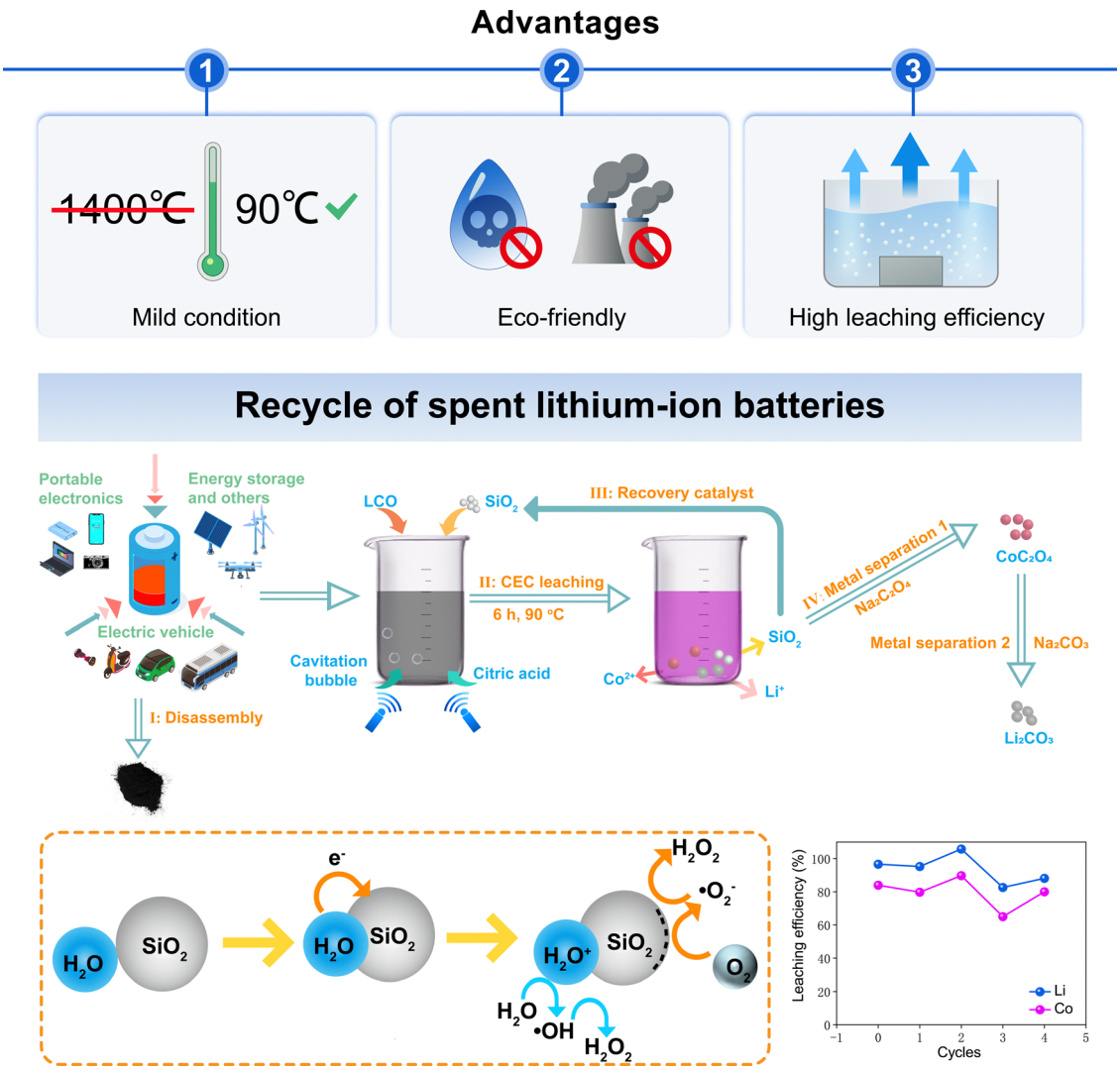

Fig. 12 Significant application of CEC: recycling of spent lithium-ion batteries. Cathode materials in spent lithium-ion batteries could be effectively recycled under mild conditions by CEC. The leaching efficiency could reach nearly 100% with minimized environmental burden. Reproduced with permission from ref. 54. Copyright 2023, Springer Nature.

Table 1 Comparison of main features of CEC and the existing catalytic techniques

Principle	Catalysts	Condition	Applications	Kinetic rate/profit	Ref.
Piezocatalysis	Bi_2WO_6	80 W/40 kHz, 80 min	Pollutant degradation	3.9×10^{-2} min^{-1}	175
Piezocatalysis	$LiNbO_3$	70 W/40 kHz, 150 min	Pollutant degradation	1.3×10^{-2} min^{-1}	176
Piezocatalysis	$BaTiO_3$	80 W/40 kHz, 160 min	Pollutant degradation	1.4×10^{-2} min^{-1}	177
Electrocatalysis	nZVC-CNT/PMS	J = 1 mL min^{-1}, V = −0.5 V	Pollutant degradation	1.20 min^{-1}	178
Photocatalysis	CDs/ZnO	125 W UV, 240 min	Pollutant degradation	3×10^{-2} min^{-1}	179
Contact-electro-catalysis	FEP	120 W/40 kHz, 180 min	Pollutant degradation	3.9×10^{-2} min^{-1}	45
Contact-electro-catalysis	PTFE	Ball milling, 350 rpm, 120 min	Pollutant degradation	4.3×10^{-2} min^{-1}	143
Piezocatalysis	BiOCl	150 W/53 kHz, 60 min	H_2O_2 production	5.6 mmol L^{-1} g^{-1} h^{-1}	180
Piezocatalysis	HAP	300 W/40 kHz, 30 min	H_2O_2 production	9.34 mmol L^{-1} g^{-1} h^{-1}	181
Piezocatalysis	BCZT-0.5	180 W/40 kHz, 14 h	H_2O_2 production	13.84 mmol L^{-1} g^{-1} h^{-1}	182
Electrocatalysis	CoPc-OCNT	O_2 supply, 100 mA cm^{-2}	H_2O_2 production	11.53 mol L^{-1} g^{-1} h^{-1}	183
Photocatalysis	MX-> PHI	O_2 supply, 150 W, 120 min	H_2O_2 production	9.79 mol L^{-1} g^{-1} h^{-1}	184
Contact-electro-catalysis	FEP	110 W/40 kHz, 60 min	H_2O_2 production	58.8 mmol L^{-1} g^{-1} h^{-1}	49
Contact-electro-catalysis	PTFE	200 W/40 kHz, 60 min	H_2O_2 production	15.65 mmol L^{-1} h^{-1}	48
Electrodeposition	PDADMA/Cu	10 M HCl, 4 g/30 mL, 2 h	LIB recycling	0.2 ($ per kg)	185
Oxidation leaching	N/A	H_2O_2, 50 °C, 30 min	LIB recycling	0.295 ($ per kg)	186
Direct recycling	N/A	0.2 M LiOH, 0.08 M CA, 90 °C	LIB recycling	1.1 ($ per kg)	187
Acid leaching	N/A	1 M H_2SO_4, 0.6 M malonic acid, 5% H_2O_2, 70 °C, 60 min	LIB recycling	8.69 ($ per kg)	188
Ball milling	N/A	Oxalic acid, 500 rpm, 2 h	LIB recycling	57.61 ($ per kg)	189
Contact-electro-catalysis	SiO_2	0.2 M CA, 70 °C, 360 min	LIB recycling	13.43 ($ per kg)	54

for catalyzing some frontier reactions that usually take place at very high temperatures. This is largely because the CEC catalysts are mainly polymers whose CE performance decreases with the increase of temperatures.[132] We suppose this challenge could be properly addressed by the development of materials that can exhibit robust CE ability even at high temperatures. Moreover, the efficiency of CEC is comparable and even superior to that of the existing mechanochemical strategies, but it is relatively sluggish in comparison with electrocatalysis or photocatalysis. Table 1 compares the main features of CEC and existing catalytic techniques from several aspects. We believe that improving the CE ability of existing materials or devising novel materials that are intrinsically suitable for CE are both effective to boost the efficiency of CEC. Alternatively, efforts for developing more effective strategies to initiate CEC should also be feasible. It is expected that the CEC could be utilized in broader application fields after addressing these challenges.

4. Summary and perspectives

The interactions between two surfaces under external mechanical forces would bring about a series of effects, and various catalytic strategies have been developed based on these effects.[190–192] Tribocatalysis has been introduced as a pivotal concept several decades ago, and mainly exploits the temperature increase or bond breakage induced by fierce friction to accelerate reaction rates.[193–195] Although the CE effect should also present in a typical tribocatalytic process, it may not play the dominant role partly because electrons will be thermionically emitted rather than exchanged at elevated temperature. In virtue of the CE-driven interfacial electron transfer, the concept of contact-electrocatalysis (CEC) has been proposed recently, which is demonstrated to be a vital and promising avenue for mechanochemical research. Because the CE effect could occur even without intense friction during contact, CEC might offer a much milder condition for promoting reaction rates.[38] In addition, catalysts used in tribocatalysis are usually metals or their oxides that should withstand high-temperatures and severe surface abrasions, while also providing active sites for catalysis.[196–198] Benefitting from the ubiquitous nature of the CE effect, CEC is capable of enriching the spectrum of available catalysts, and the catalysts are expected to exhibit superior recyclability and reusability because less damage will be caused during CEC processes. Moreover, tribocatalysis usually requires solid–solid friction pairs to induce violent frictions, thus creating suitable conditions for catalysis. CEC could eliminate such restrictions as CE also occurs at solid–gas or liquid–liquid interfaces, which enables direct electron exchange between substrates even though they are in gaseous or liquid phases.[68,131]

A representative case of liquid–liquid contact-electrification (L–L CE) takes place at oil–water interfaces,[199] and electrons are the dominant charge carrier in this situation since nearly no ion is present in these two liquids. Similar to the L–S CE, we believe that the CE at the L–L interface could also drive the corresponding electron transfer and subsequent redox reactions. For example, the perfluorocarbon (PFC) liquid is ideal for CE with water since the fluorine group in PFC could facilely grab electrons from the surrounding water molecules.[200] We suppose that electron transfer during CE between PFC and surrounding water/oxygen molecules could give rise to ROS in the same manner. Despite several fundamental differences between tribocatalysis and CEC, we expect a scenario that could combine these two catalytic strategies in one mechanochemical system and make full use of advantages from both. A comprehensive roadmap has been proposed, which summarizes priority directions and major challenges, paving the way for further advancements in the rapidly increasing field of CEC (Fig. 13).

1. Enhancing the performance of CEC catalysts

The efficiency of CEC highly depends on the CE ability of used catalysts, which highlights the necessity for developing

materials that could exhibit enhanced CE performance. Physical etching to increase the contact surface area or chemical modifications to improve the surface charge density are two representative strategies for improving the CE ability of given materials. Another effective approach involves devising novel materials that are intrinsically suitable for CE. In addition to explorations on the category of catalysts, optimizing the structure and morphology also presents significant potential for

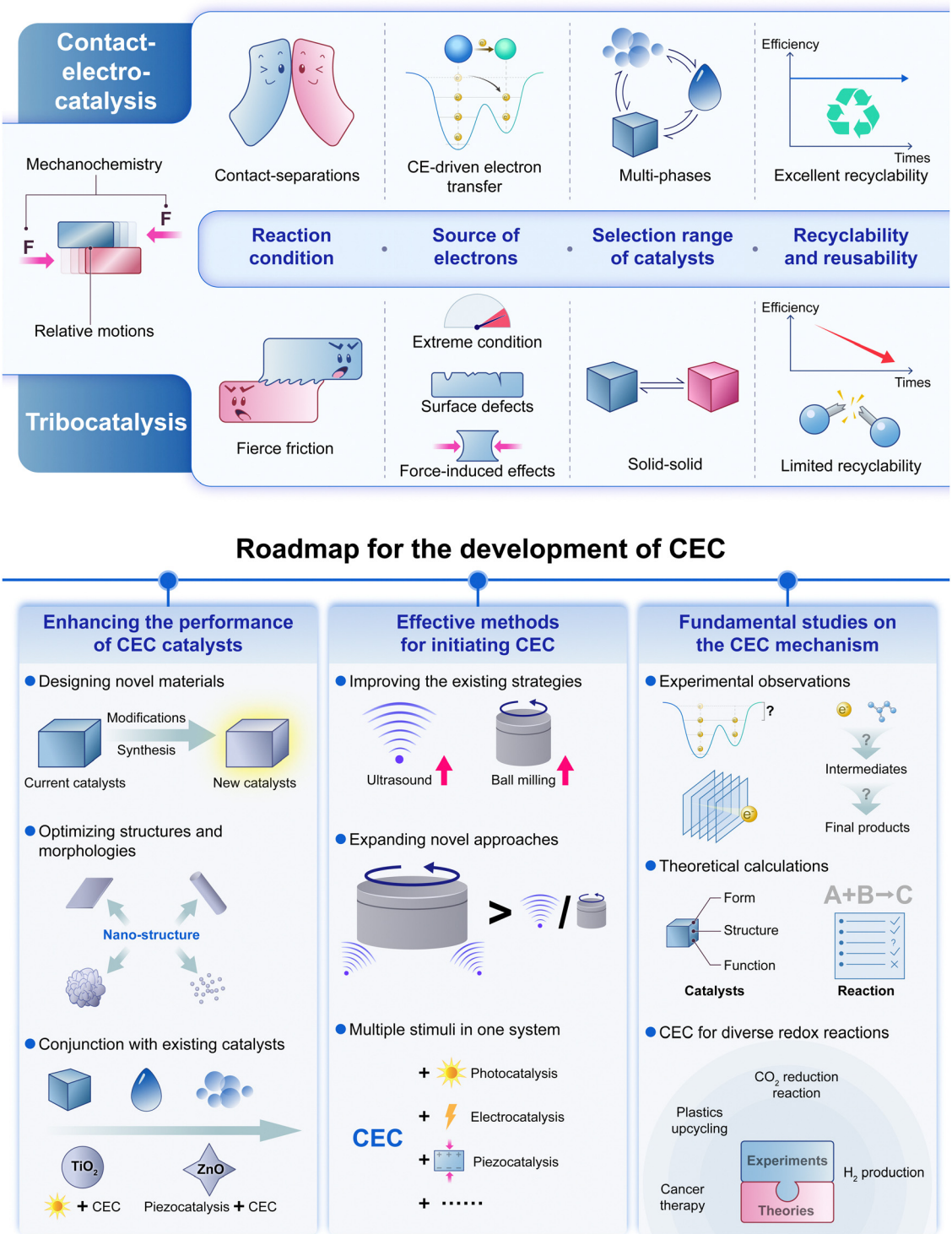

Fig. 13 The role of contact-electro-catalysis in mechanochemistry and the roadmap for its development. The similarity and disparity between tribocatalysis and contact-electro-catalysis have been discussed from several aspects. A road map for the development of CEC has been presented, which involves research frontiers from both experimental and theoretical aspects.

improving catalytic efficiency – an aspect that has been extensively investigated in conventional catalytic methods yet has not been conducted in CEC. More importantly, the ubiquity of CE could offer abundant opportunities for implementing CEC catalysts in conjunction with conventional catalysts to achieve an improved overall catalytic efficiency. This approach holds the potential as a universal strategy for boosting the performance of existing catalysts.

2. Effective methods for initiating CEC

Ultrasonication and ball milling serve as two representative approaches for initiating CEC, and their operating parameters could considerably affect the CEC efficiency. Although theoretical explanations about the potential mechanism have been proposed, there still lack direct observations and concrete evidence for elucidating how these experimental factors impact the CE process. To address this challenge, an in-depth investigation focused on specific regions to reveal how the contact-separations are induced at local spots should be helpful. Such examinations could not only guide the optimization of CEC efficiency in current strategies, but also inspire us to explore novel methods for initiating CEC in a more effective way. Moreover, the incorporation of diverse stimuli within a single system should also be considered. For instance, the collision frequency and input energy could both be improved if multiple mechanical stimuli are applied together. As a consequence, the CEC efficiency should be significantly promoted due to enhanced CE frequency and quantity of exchanged electrons. Stimuli other than mechanical agitations could also favor the improvement of CEC efficiency. Exemplified by a system that combines CEC with photocatalysis or electrocatalysis, we expect the overall catalytic efficiency could be substantially promoted by ultrasonication in the presence of light irradiation or external electricity, respectively.

3. Fundamental studies on the CEC mechanism

Mechanistic studies of CEC could provide us with a comprehensive understanding of CEC and, in turn, advancing its applications across various domains. Current research in CE mainly focuses on evaluating and enhancing the charge density on contact surfaces. However, the energy of electrons is also of great significance especially for estimating the feasibility of a catalytic process, which emphasizes the necessity for devising a reliable strategy to precisely assess the energy levels of CE-induced electrons. A quantified contact-electro-catalytic diagram could thus be established for facilitating the selection of CEC catalysts and suitable methods for catalyzing target reactions. Furthermore, a time-resolved method that could *in situ* characterize the CE-driven interfacial electron transfer process might enable us to investigate how these electrons are produced and transferred under external mechanical stimuli. After fusion with an appropriate intermediate capturing strategy, the stepwise catalytic mechanism and corresponding reaction path could be elucidated. Besides, computational investigations are also indispensable for the development of CEC. On the one hand, theoretical calculations about the composition and structure lay the foundation for designing novel catalysts with enhanced CEC efficiency. On the other hand, simulations on the catalytic process offer valuable insights into the interaction between CE-induced electrons and adsorbed molecules on surfaces. We expect that these fundamental studies could unravel the operating mechanism of CEC, thus expanding the category of feasible catalytic processes and enabling efficient catalysis for a broader spectrum of cutting-edge chemical reactions.

Conflicts of interest

All the authors declare no competing interests.

Acknowledgements

The authors would like to express their sincere gratitude to Drs. Feng-Ru Fan, Laipan Zhu, Qingxia Liu, Peng Jiang, Jun Liu, Yun-Ze Long, and many of our collaborators for their important contributions to the study of contact-electro-catalysis (CEC). The authors also acknowledge the valuable input and support provided by Drs. Yawei Feng, Site Li, Huifan Li, Jiawei Zhao, Berbille Andy, Xiao-Fen Li, and all our group members. This work is financially supported by the National Key R&D Project from Minister of Science and Technology (Grant No. 2016YFA0202704), the National Natural Science Foundation of China (Grant No. 51432005, and 5151101243), and the China Postdoctoral Science Foundation (Grant No. 2022M723101).

References

1 S. Gao, Y. Lin, X. Jiao, Y. Sun, Q. Luo, W. Zhang, D. Li, J. Yang and Y. Xie, *Nature*, 2016, **529**, 68–71.
2 C.-T. Dinh, T. Burdyny, M. G. Kibria, A. Seifitokaldani, C. M. Gabardo, F. P. García de Arquer, A. Kiani, J. P. Edwards, P. De Luna, O. S. Bushuyev, C. Zou, R. Quintero-Bermudez, Y. Pang, D. Sinton and E. H. Sargent, *Science*, 2018, **360**, 783–787.
3 Y. Chen, M. Xu, J. Wen, Y. Wan, Q. Zhao, X. Cao, Y. Ding, Z. L. Wang, H. Li and Z. Bian, *Nat. Sustainability*, 2021, **4**, 618–626.
4 X. Li, Y. Sun, J. Xu, Y. Shao, J. Wu, X. Xu, Y. Pan, H. Ju, J. Zhu and Y. Xie, *Nat. Energy*, 2019, **4**, 690–699.
5 P.-C. Chen, C. Chen, Y. Yang, A. L. Maulana, J. Jin, J. Feijoo and P. Yang, *J. Am. Chem. Soc.*, 2023, **145**, 10116–10125.
6 J. Moon, W. Beker, M. Siek, J. Kim, H. S. Lee, T. Hyeon and B. A. Grzybowski, *Nat. Mater.*, 2024, **23**, 108–115.
7 A. E. Thorarinsdottir, D. P. Erdosy, C. Costentin, J. A. Mason and D. G. Nocera, *Nat. Catal.*, 2023, **6**, 425–434.
8 L. Buzzetti, G. E. M. Crisenza and P. Melchiorre, *Angew. Chem., Int. Ed.*, 2019, **58**, 3730–3747.
9 T. von Münchow, S. Dana, Y. Xu, B. Yuan and L. Ackermann, *Science*, 2023, **379**, 1036–1042.
10 A. H. Proppe, Y. C. Li, A. Aspuru-Guzik, C. P. Berlinguette, C. J. Chang, R. Cogdell, A. G. Doyle, J. Flick, N. M. Gabor,

R. van Grondelle, S. Hammes-Schiffer, S. A. Jaffer, S. O. Kelley, M. Leclerc, K. Leo, T. E. Mallouk, P. Narang, G. S. Schlau-Cohen, G. D. Scholes, A. Vojvodic, V. W.-W. Yam, J. Y. Yang and E. H. Sargent, *Nat. Rev. Mater.*, 2020, **5**, 828–846.

11 B. Qiao, A. Wang, X. Yang, L. F. Allard, Z. Jiang, Y. Cui, J. Liu, J. Li and T. Zhang, *Nat. Chem.*, 2011, **3**, 634–641.

12 C. Xie, Z. Niu, D. Kim, M. Li and P. Yang, *Chem. Rev.*, 2020, **120**, 1184–1249.

13 T. Mou, H. S. Pillai, S. Wang, M. Wan, X. Han, N. M. Schweitzer, F. Che and H. Xin, *Nat. Catal.*, 2023, **6**, 122–136.

14 V. R. Stamenkovic, D. Strmcnik, P. P. Lopes and N. M. Markovic, *Nat. Mater.*, 2017, **16**, 57–69.

15 E. Roduner, *Chem. Soc. Rev.*, 2014, **43**, 8226–8239.

16 J. Lv, J. Xie, A. G. A. Mohamed, X. Zhang, Y. Feng, L. Jiao, E. Zhou, D. Yuan and Y. Wang, *Nat. Rev. Chem.*, 2023, **7**, 91–105.

17 A. Wang, J. Li and T. Zhang, *Nat. Rev. Chem.*, 2018, **2**, 65–81.

18 B. Zhang, X. Zheng, O. Voznyy, R. Comin, M. Bajdich, M. García-Melchor, L. Han, J. Xu, M. Liu, L. Zheng, F. P. García de Arquer, C. T. Dinh, F. Fan, M. Yuan, E. Yassitepe, N. Chen, T. Regier, P. Liu, Y. Li, P. De Luna, A. Janmohamed, H. L. Xin, H. Yang, A. Vojvodic and E. H. Sargent, *Science*, 2016, **352**, 333–337.

19 Z. Wang, C. Li and K. Domen, *Chem. Soc. Rev.*, 2019, **48**, 2109–2125.

20 M. Yoon, Y. Dong, Y. Huang, B. Wang, J. Kim, J.-S. Park, J. Hwang, J. Park, S. J. Kang, J. Cho and J. Li, *Nat. Energy*, 2023, **8**, 482–491.

21 Z. Chen, J. A. M. Mercer, X. Zhu, J. A. H. Romaniuk, R. Pfattner, L. Cegelski, T. J. Martinez, N. Z. Burns and Y. Xia, *Science*, 2017, **357**, 475–479.

22 Y. Hu, B. Li, C. Yu, H. Fang and Z. Li, *Mater. Today*, 2023, **63**, 288–312.

23 D. Cao, X. Sun, Y. Li, A. Anderson, W. Lu and H. Zhu, *Adv. Mater.*, 2022, **34**, 2200401.

24 K. Kubota, Y. Pang, A. Miura and H. Ito, *Science*, 2019, **366**, 1500–1504.

25 T. Friščić, C. Mottillo and H. M. Titi, *Angew. Chem., Int. Ed.*, 2020, **59**, 1018–1029.

26 G.-F. Han, F. Li, Z.-W. Chen, C. Coppex, S.-J. Kim, H.-J. Noh, Z. Fu, Y. Lu, C. V. Singh, S. Siahrostami, Q. Jiang and J.-B. Baek, *Nat. Nanotechnol.*, 2021, **16**, 325–330.

27 Z. Li, C. Mao, Q. Pei, P. N. Duchesne, T. He, M. Xia, J. Wang, L. Wang, R. Song, A. A. Jelle, D. M. Meira, Q. Ge, K. K. Ghuman, L. He, X. Zhang and G. A. Ozin, *Nat. Commun.*, 2022, **13**, 7205.

28 L. Chen, J. Wen, P. Zhang, B. Yu, C. Chen, T. Ma, X. Lu, S. H. Kim and L. Qian, *Nat. Commun.*, 2018, **9**, 1542.

29 S. Akbulatov, Y. Tian, Z. Huang, T. J. Kucharski, Q.-Z. Yang and R. Boulatov, *Science*, 2017, **357**, 299–303.

30 X. Liao, H. Xie, B. Liao, S. Hou, Y. Yu and X. Fan, *Nano Energy*, 2022, **94**, 106890.

31 H. Xia and Z. Wang, *Science*, 2019, **366**, 1451–1452.

32 S. Lin, L. Xu, A. Chi Wang and Z. L. Wang, *Nat. Commun.*, 2020, **11**, 399.

33 J. Nie, Z. Ren, L. Xu, S. Lin, F. Zhan, X. Chen and Z. L. Wang, *Adv. Mater.*, 2020, **32**, 1905696.

34 S. Lin, X. Chen and Z. L. Wang, *Chem. Rev.*, 2022, **122**, 5209–5232.

35 S. Lin, L. Xu, C. Xu, X. Chen, A. C. Wang, B. Zhang, P. Lin, Y. Yang, H. Zhao and Z. L. Wang, *Adv. Mater.*, 2019, **31**, 1808197.

36 F. Zhan, A. C. Wang, L. Xu, S. Lin, J. Shao, X. Chen and Z. L. Wang, *ACS Nano*, 2020, **14**, 17565–17573.

37 C. Xu, Y. Zi, A. C. Wang, H. Zou, Y. Dai, X. He, P. Wang, Y.-C. Wang, P. Feng, D. Li and Z. L. Wang, *Adv. Mater.*, 2018, **30**, 1706790.

38 Z. L. Wang and A. C. Wang, *Mater. Today*, 2019, **30**, 34–51.

39 S. Lin, X. Chen and Z. L. Wang, *Nano Energy*, 2020, **76**, 105070.

40 F. Galembeck, T. A. Burgo, L. B. Balestrin, R. F. Gouveia, C. A. Silva and A. Galembeck, *RSC Adv.*, 2014, **4**, 64280–64298.

41 L. P. Santos, D. Lermen, R. G. Yoshimura, B. L. da Silva, A. Galembeck, T. A. L. Burgo and F. Galembeck, *Langmuir*, 2023, **39**, 5840–5850.

42 X. Chen, Y. Xia, Z. Zhang, L. Hua, X. Jia, F. Wang and R. N. Zare, *J. Am. Chem. Soc.*, 2023, **145**, 21538–21545.

43 A. J. Colussi, *J. Am. Chem. Soc.*, 2023, **145**, 16315–16317.

44 M. A. Mehrgardi, M. Mofidfar and R. N. Zare, *J. Am. Chem. Soc.*, 2022, **144**, 7606–7609.

45 Z. Wang, A. Berbille, Y. Feng, S. Li, L. Zhu, W. Tang and Z. L. Wang, *Nat. Commun.*, 2022, **13**, 130.

46 H. Zou, Y. Zhang, L. Guo, P. Wang, X. He, G. Dai, H. Zheng, C. Chen, A. C. Wang, C. Xu and Z. L. Wang, *Nat. Commun.*, 2019, **10**, 1427.

47 H. Zou, L. Guo, H. Xue, Y. Zhang, X. Shen, X. Liu, P. Wang, X. He, G. Dai, P. Jiang, H. Zheng, B. Zhang, C. Xu and Z. L. Wang, *Nat. Commun.*, 2020, **11**, 2093.

48 J. Zhao, X. Zhang, J. Xu, W. Tang, Z. Lin Wang and F. Ru Fan, *Angew. Chem.*, 2023, **135**, e202300604.

49 A. Berbille, X. F. Li, Y. Su, S. Li, X. Zhao, L. Zhu and Z. L. Wang, *Adv. Mater.*, 2023, **35**, 2304387.

50 X. Zhao, Y. Su, A. Berbille, Z. L. Wang and W. Tang, *Nanoscale*, 2023, **15**, 6243–6251.

51 S. Lin, C. Xu, L. Xu and Z. L. Wang, *Adv. Funct. Mater.*, 2020, **30**, 1909724.

52 Z. Tang, S. Lin and Z. L. Wang, *Adv. Mater.*, 2021, **33**, 2102886.

53 Z. Wang, J. An, J. Nie, J. Luo, J. Shao, T. Jiang, B. Chen, W. Tang and Z. L. Wang, *Adv. Mater.*, 2020, **32**, 2001466.

54 H. Li, A. Berbille, X. Zhao, Z. Wang, W. Tang and Z. L. Wang, *Nat. Energy*, 2023, **8**, 1137–1144.

55 A. Abdal Dayem, M. K. Hossain, S. B. Lee, K. Kim, S. K. Saha, G.-M. Yang, H. Y. Choi and S.-G. Cho, *Int. J. Mol. Sci.*, 2017, **18**, 120.

56 D. B. Graves, *J. Phys. D*, 2012, **45**, 263001.

57 B. Yang, Y. Chen and J. Shi, *Chem. Rev.*, 2019, **119**, 4881–4985.

58 M. P. Murphy, H. Bayir, V. Belousov, C. J. Chang, K. J. A. Davies, M. J. Davies, T. P. Dick, T. Finkel,

H. J. Forman, Y. Janssen-Heininger, D. Gems, V. E. Kagan, B. Kalyanaraman, N.-G. Larsson, G. L. Milne, T. Nyström, H. E. Poulsen, R. Radi, H. Van Remmen, P. T. Schumacker, P. J. Thornalley, S. Toyokuni, C. C. Winterbourn, H. Yin and B. Halliwell, *Nat. Metab.*, 2022, **4**, 651–662.

59 H. Guo, X. Pu, J. Chen, Y. Meng, M.-H. Yeh, G. Liu, Q. Tang, B. Chen, D. Liu, S. Qi, C. Wu, C. Hu, J. Wang and Z. L. Wang, *Sci. Robot.*, 2018, **3**, eaat2516.

60 W. Tang, T. Jiang, F. R. Fan, A. F. Yu, C. Zhang, X. Cao and Z. L. Wang, *Adv. Funct. Mater.*, 2015, **25**, 3718–3725.

61 J. Nie, Z. Wang, Z. Ren, S. Li, X. Chen and Z. Lin Wang, *Nat. Commun.*, 2019, **10**, 2264.

62 Z. Ren, Z. Wang, Z. Liu, L. Wang, H. Guo, L. Li, S. Li, X. Chen, W. Tang and Z. L. Wang, *Adv. Energy Mater.*, 2020, **10**, 2001770.

63 J. Luo, Z. Wang, L. Xu, A. C. Wang, K. Han, T. Jiang, Q. Lai, Y. Bai, W. Tang, F. R. Fan and Z. L. Wang, *Nat. Commun.*, 2019, **10**, 5147.

64 S. Lin, L. Zhu, Z. Tang and Z. L. Wang, *Nat. Commun.*, 2022, **13**, 5230.

65 T. A. Gmür, A. Goel and M. A. Brown, *J. Phys. Chem. C*, 2016, **120**, 16617–16625.

66 J. Zhang, S. Lin and Z. L. Wang, *ACS Nano*, 2023, **17**, 1646–1652.

67 X. Zhao, X. Lu, Q. Zheng, L. Fang, L. Zheng, X. Chen and Z. L. Wang, *Nano Energy*, 2021, **87**, 106191.

68 H. Qin, L. Xu, F. Zhan and Z. L. Wang, *Nano Energy*, 2023, **116**, 108762.

69 C. Tan, R. Xu and Q. Zhang, *Langmuir*, 2022, **38**, 11882–11891.

70 S. Li, J. Nie, Y. Shi, X. Tao, F. Wang, J. Tian, S. Lin, X. Chen and Z. L. Wang, *Adv. Mater.*, 2020, **32**, 2001307.

71 Y. Liu, Q. Fu, J. Mo, Y. Lu, C. Cai, B. Luo and S. Nie, *Nano Energy*, 2021, **89**, 106369.

72 X. Tao, J. Nie, S. Li, Y. Shi, S. Lin, X. Chen and Z. L. Wang, *ACS Nano*, 2021, **15**, 10609–10617.

73 S. Lin, M. Zheng, J. Luo and Z. L. Wang, *ACS Nano*, 2020, **14**, 10733–10741.

74 C. Xu, B. Zhang, A. C. Wang, H. Zou, G. Liu, W. Ding, C. Wu, M. Ma, P. Feng, Z. Lin and Z. L. Wang, *ACS Nano*, 2019, **13**, 2034–2041.

75 C. Xu, B. Zhang, A. C. Wang, W. Cai, Y. Zi, P. Feng and Z. L. Wang, *Adv. Funct. Mater.*, 2019, **29**, 1903142.

76 A. C. Wang, B. Zhang, C. Xu, H. Zou, Z. Lin and Z. L. Wang, *Adv. Funct. Mater.*, 2020, **30**, 1909384.

77 J. Zhang, S. Lin, M. Zheng and Z. L. Wang, *ACS Nano*, 2021, **15**, 14830–14837.

78 S. Lin and Z. L. Wang, *Appl. Phys. Lett.*, 2021, **118**, 193901.

79 J. An, Z. M. Wang, T. Jiang, X. Liang and Z. L. Wang, *Adv. Funct. Mater.*, 2019, **29**, 1904867.

80 J. An, Z. Wang, T. Jiang, P. Chen, X. Liang, J. Shao, J. Nie, M. Xu and Z. L. Wang, *Mater. Today*, 2020, **41**, 10–20.

81 X. Liu, J. Zhang, X. Wang, S. Lin and Z. L. Wang, *J. Mater. Chem. A*, 2023, **11**, 18964–18971.

82 X. Wang, J. Zhang, X. Liu, S. Lin and Z. L. Wang, *J. Mater. Chem. A*, 2023, **11**, 5696–5702.

83 S. Lin, L. Xu, L. Zhu, X. Chen and Z. L. Wang, *Adv. Mater.*, 2019, **31**, 1901418.

84 Z. Zhang, N. Yin, Z. Wu, S. Pan and D. Wang, *Nano Energy*, 2021, **79**, 105501.

85 Y. Nan, J. Shao, M. Willatzen and Z. L. Wang, *Research*, 2022, **2022**, 9861463.

86 M. Willatzen and Z. L. Wang, *Research*, 2019, **2019**, 6528689.

87 J.-W. Lee and W. Hwang, *Nano Energy*, 2018, **52**, 315–322.

88 L. Li, X. Wang, P. Zhu, H. Li, F. Wang and J. Wu, *Nano Energy*, 2020, **70**, 104476.

89 M. Willatzen, L. C. Lew Yan Voon and Z. L. Wang, *Adv. Funct. Mater.*, 2020, **30**, 1910461.

90 M. Sun, Q. Lu, Z. L. Wang and B. Huang, *Nat. Commun.*, 2021, **12**, 1752.

91 S. S. P. Parkin, C. Kaiser, A. Panchula, P. M. Rice, B. Hughes, M. Samant and S.-H. Yang, *Nat. Mater.*, 2004, **3**, 862–867.

92 S. A. Wolf, D. D. Awschalom, R. A. Buhrman, J. M. Daughton, S. von Molnár, M. L. Roukes, A. Y. Chtchelkanova and D. M. Treger, *Science*, 2001, **294**, 1488–1495.

93 A. D. Lorenzo and Y. V. Nazarov, *Phys. Rev. Lett.*, 2005, **94**, 210601.

94 A. L. Buchachenko and V. L. Berdinsky, *Chem. Rev.*, 2002, **102**, 603–612.

95 K. Maeda, K. B. Henbest, F. Cintolesi, I. Kuprov, C. T. Rodgers, P. A. Liddell, D. Gust, C. R. Timmel and P. J. Hore, *Nature*, 2008, **453**, 387–390.

96 B. Brocklehurst, *Chem. Soc. Rev.*, 2002, **31**, 301–311.

97 J. Zhang, S. Lin and Z. L. Wang, *J. Phys. Chem. B*, 2022, **126**, 2754–2760.

98 W. Schmickler, *Chem. Rev.*, 1996, **96**, 3177–3200.

99 S.-J. Shin, D. H. Kim, G. Bae, S. Ringe, H. Choi, H.-K. Lim, C. H. Choi and H. Kim, *Nat. Commun.*, 2022, **13**, 174.

100 G. Gonella, E. H. G. Backus, Y. Nagata, D. J. Bonthuis, P. Loche, A. Schlaich, R. R. Netz, A. Kühnle, I. T. McCrum, M. T. M. Koper, M. Wolf, B. Winter, G. Meijer, R. K. Campen and M. Bonn, *Nat. Rev. Chem.*, 2021, **5**, 466–485.

101 D. Choi, D. W. Kim, D. Yoo, K. J. Cha, M. La and D. S. Kim, *Nano Energy*, 2017, **36**, 250–259.

102 Z. Chen, Y. Lu, R. Li, D. Li, B. Xiang, J. Li and Q. Liu, *Nano Energy*, 2023, **116**, 108834.

103 W. Xu, H. Zheng, Y. Liu, X. Zhou, C. Zhang, Y. Song, X. Deng, M. Leung, Z. Yang, R. X. Xu, Z. L. Wang, X. C. Zeng and Z. Wang, *Nature*, 2020, **578**, 392–396.

104 L. L. Zhang and X. Zhao, *Chem. Soc. Rev.*, 2009, **38**, 2520–2531.

105 Z. Adamczyk and P. Warszyński, *Adv. Colloid Interface Sci.*, 1996, **63**, 41–149.

106 K. Zhao and K. He, *Phys. Rev. B*, 2006, **74**, 205319.

107 T. Fujimoto and K. Awaga, *Phys. Chem. Chem. Phys.*, 2013, **15**, 8983–9006.

108 B. R. Boswell, C. M. F. Mansson, J. M. Cox, Z. Jin, J. A. H. Romaniuk, K. P. Lindquist, L. Cegelski, Y. Xia, S. A. Lopez and N. Z. Burns, *Nat. Chem.*, 2021, **13**, 41–46.

109 S. Chen, Y. Liu and J. Chen, *Chem. Soc. Rev.*, 2014, **43**, 5372–5386.

110 D. Bohra, J. H. Chaudhry, T. Burdyny, E. A. Pidko and W. A. Smith, *Energy Environ. Sci.*, 2019, **12**, 3380–3389.
111 C.-L. Wang, J. Wang, J.-K. Jin, B. Li, Y. L. Phang, F.-L. Zhang, T. Ye, H.-M. Xia, L.-W. Hui, J.-H. Su, Y. Fu and Y.-F. Wang, *Science*, 2023, **382**, 1056–1065.
112 Y. Chen, X.-Y. Li, Z. Chen, A. Ozden, J. E. Huang, P. Ou, J. Dong, J. Zhang, C. Tian, B.-H. Lee, X. Wang, S. Liu, Q. Qu, S. Wang, Y. Xu, R. K. Miao, Y. Zhao, Y. Liu, C. Qiu, J. Abed, H. Liu, H. Shin, D. Wang, Y. Li, D. Sinton and E. H. Sargent, *Nat. Nanotechnol.*, 2023, 1–8.
113 C.-X. Zhao, J.-N. Liu, J. Wang, C. Wang, X. Guo, X.-Y. Li, X. Chen, L. Song, B.-Q. Li and Q. Zhang, *Sci. Adv.*, 2022, **8**, eabn5091.
114 T. He, W. Wang, F. Shi, X. Yang, X. Li, J. Wu, Y. Yin and M. Jin, *Nature*, 2021, **598**, 76–81.
115 J. Jin, J. Wicks, Q. Min, J. Li, Y. Hu, J. Ma, Y. Wang, Z. Jiang, Y. Xu, R. Lu, G. Si, P. Papangelakis, M. Shakouri, Q. Xiao, P. Ou, X. Wang, Z. Chen, W. Zhang, K. Yu, J. Song, X. Jiang, P. Qiu, Y. Lou, D. Wu, Y. Mao, A. Ozden, C. Wang, B. Y. Xia, X. Hu, V. P. Dravid, Y.-M. Yiu, T.-K. Sham, Z. Wang, D. Sinton, L. Mai, E. H. Sargent and Y. Pang, *Nature*, 2023, **617**, 724–729.
116 Y. Ma, X. Wang, Y. Jia, X. Chen, H. Han and C. Li, *Chem. Rev.*, 2014, **114**, 9987–10043.
117 Z. C. Litman, Y. Wang, H. Zhao and J. F. Hartwig, *Nature*, 2018, **560**, 355–359.
118 X. Huang, B. Wang, Y. Wang, G. Jiang, J. Feng and H. Zhao, *Nature*, 2020, **584**, 69–74.
119 S. Shaik, R. Ramanan, D. Danovich and D. Mandal, *Chem. Soc. Rev.*, 2018, **47**, 5125–5145.
120 X. Du, J. Huang, J. Zhang, Y. Yan, C. Wu, Y. Hu, C. Yan, T. Lei, W. Chen, C. Fan and J. Xiong, *Angew. Chem., Int. Ed.*, 2019, **58**, 4484–4502.
121 X. Song, Y. Meng and R. N. Zare, *J. Am. Chem. Soc.*, 2022, **144**, 16744–16748.
122 X. Song, C. Basheer, Y. Xia, J. Li, I. Abdulazeez, A. A. Al-Saadi, M. Mofidfar, M. A. Suliman and R. N. Zare, *J. Am. Chem. Soc.*, 2023, **145**, 25910–25916.
123 B. Chen, Y. Xia, R. He, H. Sang, W. Zhang, J. Li, L. Chen, P. Wang, S. Guo and Y. Yin, *Proc. Natl. Acad. Sci. U. S. A.*, 2022, **119**, e2209056119.
124 S. Lin, L. N. Y. Cao, Z. Tang and Z. L. Wang, *Proc. Natl. Acad. Sci. U. S. A.*, 2023, **120**, e2307977120.
125 J. Ma, F. Wang and M. Mostafavi, *Molecules*, 2018, **23**, 244.
126 Z.-H. Loh, G. Doumy, C. Arnold, L. Kjellsson, S. H. Southworth, A. Al Haddad, Y. Kumagai, M.-F. Tu, P. J. Ho, A. M. March, R. D. Schaller, M. S. Bin Mohd Yusof, T. Debnath, M. Simon, R. Welsch, L. Inhester, K. Khalili, K. Nanda, A. I. Krylov, S. Moeller, G. Coslovich, J. Koralek, M. P. Minitti, W. F. Schlotter, J.-E. Rubensson, R. Santra and L. Young, *Science*, 2020, **367**, 179–182.
127 Y. Gauduel, S. Pommeret, A. Migus and A. Antonetti, *Chem. Phys.*, 1990, **149**, 1–10.
128 X. Pu, H. Guo, J. Chen, X. Wang, Y. Xi, C. Hu and Z. L. Wang, *Sci. Adv.*, 2017, **3**, e1700694.
129 S. Chatterjee, S. Saha, S. R. Barman, I. Khan, Y.-P. Pao, S. Lee, D. Choi and Z.-H. Lin, *Nano Energy*, 2020, **77**, 105093.
130 C.-D. Le, C.-P. Vo, T.-H. Nguyen, D.-L. Vu and K. K. Ahn, *Nano Energy*, 2021, **80**, 105571.
131 L. Sun, Z. Wang, C. Li, W. Tang and Z. Wang, *Nanoenergy Adv.*, 2023, **3**, 1–11.
132 X. Dong, Z. Wang, A. Berbille, X. Zhao, W. Tang and Z. L. Wang, *Nano Energy*, 2022, **99**, 107346.
133 Z. Chen, Y. Lu, X. Liu, J. Li and Q. Liu, *Nano Energy*, 2023, **108**, 108198.
134 L. Lin, V. G. N. Thyagaraja, R. Ranjith, R. Yang, S. Ciampi, J. Chen and J. Liu, *Nano Energy*, 2023, **107**, 108163.
135 S. Lin and Z. Lin Wang, *Mater. Today*, 2023, **62**, 111–128.
136 Z. Zhang, D. Jiang, J. Zhao, G. Liu, T. Bu, C. Zhang and Z. L. Wang, *Adv. Energy Mater.*, 2020, **10**, 1903713.
137 M. Zheng, S. Lin, L. Xu, L. Zhu and Z. L. Wang, *Adv. Mater.*, 2020, **32**, 2000928.
138 A. H. Chughtai, N. Ahmad, H. A. Younus, A. Laypkov and F. Verpoort, *Chem. Soc. Rev.*, 2015, **44**, 6804–6849.
139 L. Jiao, Y. Wang, H.-L. Jiang and Q. Xu, *Adv. Mater.*, 2018, **30**, 1703663.
140 A. Corma, H. García and F. X. Llabrés i Xamena, *Chem. Rev.*, 2010, **110**, 4606–4655.
141 Y. Zhang, T. Kang, X. Han, W. Yang, W. Gong, K. Li and Y. Guo, *Nano Energy*, 2023, **111**, 108433.
142 B. Jiang, X. Xue, Z. Mu, H. Zhang, F. Li, K. Liu, W. Wang, Y. Zhang, W. Li and C. Yang, *Molecules*, 2022, **27**, 8579.
143 Z. Wang, X. Dong, X.-F. Li, Y. Feng, S. Li, W. Tang and Z. L. Wang, *Nat. Commun.*, 2024, **15**, 757.
144 W.-Z. Song, M. Zhang, H.-J. Qiu, C.-L. Li, T. Chen, L.-L. Jiang, M. Yu, S. Ramakrishna, Z.-L. Wang and Y.-Z. Long, *Water Res.*, 2022, **226**, 119242.
145 M. Zhang, W.-Z. Song, T. Chen, D.-J. Sun, D.-S. Zhang, C.-L. Li, R. Li, J. Zhang, S. Ramakrishna and Y.-Z. Long, *Nano Energy*, 2023, **110**, 108329.
146 Y. Zhao, Y. Liu, Y. Wang, S. Li, Y. Liu, Z. L. Wang and P. Jiang, *Nano Energy*, 2023, **112**, 108464.
147 N. Tsochatzidis, P. Guiraud, A. Wilhelm and H. Delmas, *Chem. Eng. Sci.*, 2001, **56**, 1831–1840.
148 S. Merouani, O. Hamdaoui, Y. Rezgui and M. Guemini, *Ultrason. Sonochem.*, 2013, **20**, 815–819.
149 P. Chattopadhyay, I. Manna, S. Talapatra and S. Pabi, *Mater. Chem. Phys.*, 2001, **68**, 85–94.
150 T. Cheng, J. Shao and Z. L. Wang, *Nat. Rev. Methods Primers*, 2023, **3**, 39.
151 Y. Xia, M. Zhang, D. C. Tsang, N. Geng, D. Lu, L. Zhu, A. D. Igalavithana, P. D. Dissanayake, J. Rinklebe and X. Yang, *Appl. Biol. Chem.*, 2020, **63**, 1–13.
152 L. Ritter, K. Solomon, P. Sibley, K. Hall, P. Keen, G. Mattu and B. Linton, *J. Toxicol. Environ. Health, Part A*, 2002, **65**, 1–142.
153 J. Xu, X. Zheng, Z. Feng, Z. Lu, Z. Zhang, W. Huang, Y. Li, D. Vuckovic, Y. Li, S. Dai, G. Chen, K. Wang, H. Wang, J. K. Chen, W. Mitch and Y. Cui, *Nat. Sustainability*, 2021, **4**, 233–241.
154 B. C. Hodges, E. L. Cates and J.-H. Kim, *Nat. Nanotechnol.*, 2018, **13**, 642–650.
155 K. Mase, M. Yoneda, Y. Yamada and S. Fukuzumi, *Nat. Commun.*, 2016, **7**, 11470.

156 N. Agarwal, S. J. Freakley, R. U. McVicker, S. M. Althahban, N. Dimitratos, Q. He, D. J. Morgan, R. L. Jenkins, D. J. Willock, S. H. Taylor, C. J. Kiely and G. J. Hutchings, *Science*, 2017, **358**, 223–227.
157 R. Hage and A. Lienke, *Angew. Chem., Int. Ed.*, 2006, **45**, 206–222.
158 R. Ciriminna, L. Albanese, F. Meneguzzo and M. Pagliaro, *ChemSusChem*, 2016, **9**, 3374–3381.
159 W. Fan, B. Zhang, X. Wang, W. Ma, D. Li, Z. Wang, M. Dupuis, J. Shi, S. Liao and C. Li, *Energy Environ. Sci.*, 2020, **13**, 238–245.
160 H. Hou, X. Zeng and X. Zhang, *Angew. Chem., Int. Ed.*, 2020, **59**, 17356–17376.
161 Y. Ding, S. Maitra, S. Halder, C. Wang, R. Zheng, T. Barakat, S. Roy, L.-H. Chen and B.-L. Su, *Matter*, 2022, **5**, 2119–2167.
162 A. Merchant, S. Batzner, S. S. Schoenholz, M. Aykol, G. Cheon and E. D. Cubuk, *Nature*, 2023, **624**, 80–85.
163 L. Wang, T. Liu, T. Wu and J. Lu, *Nature*, 2022, **611**, 61–67.
164 R. Zhang, C. Wang, P. Zou, R. Lin, L. Ma, L. Yin, T. Li, W. Xu, H. Jia, Q. Li, S. Sainio, K. Kisslinger, S. E. Trask, S. N. Ehrlich, Y. Yang, A. M. Kiss, M. Ge, B. J. Polzin, S. J. Lee, W. Xu, Y. Ren and H. L. Xin, *Nature*, 2022, **610**, 67–73.
165 J. Xu, J. Zhang, T. P. Pollard, Q. Li, S. Tan, S. Hou, H. Wan, F. Chen, H. He, E. Hu, K. Xu, X.-Q. Yang, O. Borodin and C. Wang, *Nature*, 2023, **614**, 694–700.
166 M. Armand and J. M. Tarascon, *Nature*, 2008, **451**, 652–657.
167 G. Harper, R. Sommerville, E. Kendrick, L. Driscoll, P. Slater, R. Stolkin, A. Walton, P. Christensen, O. Heidrich, S. Lambert, A. Abbott, K. Ryder, L. Gaines and P. Anderson, *Nature*, 2019, **575**, 75–86.
168 T. Raj, K. Chandrasekhar, A. N. Kumar, P. Sharma, A. Pandey, M. Jang, B.-H. Jeon, S. Varjani and S.-H. Kim, *J. Hazard. Mater.*, 2022, **429**, 128312.
169 S. Zhou, Y. Zhang, Q. Meng, P. Dong, Z. Fei and Q. Li, *J. Environ. Manage.*, 2021, **277**, 111426.
170 S. P. Barik, G. Prabaharan and L. Kumar, *J. Cleaner Prod.*, 2017, **147**, 37–43.
171 X. Chen, H. Ma, C. Luo and T. Zhou, *J. Hazard. Mater.*, 2017, **326**, 77–86.
172 H. Yang, R. M. Villani, H. Wang, M. J. Simpson, M. S. Roberts, M. Tang and X. Liang, *J. Exp. Clin. Cancer Res.*, 2018, **37**, 266.
173 G.-Y. Liou and P. Storz, *Free Radic. Res.*, 2010, **44**, 479–496.
174 H. Nakamura and K. Takada, *Cancer Sci.*, 2021, **112**, 3945–3952.
175 Z. Kang, N. Qin, E. Lin, J. Wu, B. Yuan and D. Bao, *J. Cleaner Prod.*, 2020, **261**, 121125.
176 G. Singh, M. Sharma and R. Vaish, *Commun. Mater.*, 2020, **1**, 100.
177 J. Wu, N. Qin and D. Bao, *Nano Energy*, 2018, **45**, 44–51.
178 W. Zheng, Y. Liu, W. Liu, H. Ji, F. Li, C. Shen, X. Fang, X. Li and X. Duan, *Water Res.*, 2021, **194**, 116961.
179 D. Nugroho, K. Wannakan, S. Nanan and R. Benchawattananon, *Sci. Rep.*, 2024, **14**, 2455.
180 D. Shao, L. Zhang, S. Sun and W. Wang, *ChemSusChem*, 2018, **11**, 527–531.
181 G. Yin, C. Fu, F. Zhang, T. Wu, S. Hao, C. Wang and Q. Song, *J. Alloys Compd.*, 2023, **937**, 168382.
182 K. Wang, M. Zhang, D. Li, L. Liu, Z. Shao, X. Li, H. Arandiyan and S. Liu, *Nano Energy*, 2022, **98**, 107251.
183 P. Cao, X. Quan, X. Nie, K. Zhao, Y. Liu, S. Chen, H. Yu and J. G. Chen, *Nat. Commun.*, 2023, **14**, 172.
184 P. Sharma, T. J. A. Slater, M. Sharma, M. Bowker and C. R. A. Catlow, *Chem. Mater.*, 2022, **34**, 5511–5521.
185 K. Kim, D. Raymond, R. Candeago and X. Su, *Nat. Commun.*, 2021, **12**, 6554.
186 X. Qiu, B. Zhang, Y. Xu, J. Hu, W. Deng, G. Zou, H. Hou, Y. Yang, W. Sun and Y. Hu, *Green Chem.*, 2022, **24**, 2506–2515.
187 P. Xu, Q. Dai, H. Gao, H. Liu, M. Zhang, M. Li, Y. Chen, K. An, Y. S. Meng and P. Liu, *Joule*, 2020, **4**, 2609–2626.
188 P. Li, S.-h Luo, F. Su, L. Zhang, S. Yan, X. Lei, W. Mu, Q. Wang, Y. Zhang, X. Liu and P. Hou, *ACS Appl. Mater. Interfaces*, 2022, **14**, 11359–11374.
189 E. Fan, L. Li, X. Zhang, Y. Bian, Q. Xue, J. Wu, F. Wu and R. Chen, *ACS Sustainable Chem. Eng.*, 2018, **6**, 11029–11035.
190 K. Kubota and H. Ito, *Trends Chem.*, 2020, **2**, 1066–1081.
191 C. Wang, R. Zhao, W. Fan, L. Li, H. Feng, Z. Li, C. Yan, X. Shao, K. Matyjaszewski and Z. Wang, *Angew. Chem., Int. Ed.*, 2023, e202309440.
192 Y. Pang, J. W. Lee, K. Kubota and H. Ito, *Angew. Chem., Int. Ed.*, 2020, **59**, 22570–22576.
193 C. Kajdas, A. Kulczycki and D. Ozimina, *Tribol. Int.*, 2017, **107**, 144–151.
194 K. Hiratsuka, T. Abe and C. Kajdas, *Tribol. Int.*, 2010, **43**, 1659–1664.
195 C. K. Kajdas, *Tribol. Int.*, 2005, **38**, 337–353.
196 K. I. Hiratsuka, C. Kajdas and M. Yoshida, *Tribol. Trans.*, 2004, **47**, 86–93.
197 W. Song, J. Li, C. Zeng, C. Ouyang, S. Sun, K. Wang, J. Li and J. Luo, *Tribol. Int.*, 2023, **185**, 108541.
198 D. Yang, X. Liu and Y. Tian, *Tribol. Int.*, 2022, **167**, 107374.
199 P. Jiang, L. Zhang, H. Guo, C. Chen, C. Wu, S. Zhang and Z. L. Wang, *Adv. Mater.*, 2019, **31**, 1902793.
200 H. Li, Z. Wang, X. Chu, Y. Zhao, G. He, Y. Hu, Y. Liu, Z. L. Wang and P. Jiang, *J. Am. Chem. Soc.*, 2024, accepted.